

REMOTE SENSING LABORATORY



AD-A147 384

DESIGN OF AN ANALOG SPECTRUM ANALYZER  
FOR PROBING EXPERIMENTS

DTIC FILE COPY

NOV 13 1984

APPROVED FOR PUBLIC  
RELEASE DIST. UNLIMITED

THE UNIVERSITY OF KANSAS CENTER FOR RESEARCH, INC.  
2291 Irving Hill Drive-Campus West Lawrence, Kansas 66045

920 REPRODUCED AT GOVERNMENT EXPENSE 84 11 09 076

**DESIGN OF AN ANALOG SPECTRUM ANALYZER  
FOR PROBING EXPERIMENTS**

R. Zoughi  
R.K. Moore  
R.G. Onstott

Remote Sensing Laboratory  
Center for Research, Inc.  
The University of Kansas  
Lawrence, Kansas 66045-2969

RSL Technical Report  
RSL TR 3311-1

July 1984

Supported by:

OFFICE OF NAVAL RESEARCH  
Department of the Navy  
800 N. Quincy Street  
Arlington, Virginia 22217

Contract N00014-76-C-1105

NOV 13 1984

**A**

**APPROVED FOR PUBLIC  
RELEASE UNLIMITED**

**ABSTRACT.....1**

**1.0 INTRODUCTION.....1**

1.1 The FM-CW Radar.....2

1.2 FM-CW vs Impulse Radar.....4

1.3 Location of Target Response in Frequency Spectrum.....5

1.4 Penetration Depth.....9

**2.0 SPECTRAL MEASUREMENTS AND SPECTRUM ANALYSIS.....11**

2.1 Scanning Spectrum Analyzer.....11

2.2 Filter Bandwidth and Resolution.....15

**3.0 SPECTRUM ANALYZER DESIGN.....20**

3.1 Description of the Spectrum Analyzer.....20

3.2 Parameter Selections and Design Considerations.....21

3.2.1 Resolution Bandwidth.....21

3.2.2 Sweep Rate.....22

3.2.3 Gain Between Stages.....22

3.2.4 Construction Considerations.....23

3.3 Pre-Amplifier.....23

3.4 Voltage-Controlled Oscillator.....27

3.5 Sweep Generator.....29

3.6 VCO Input Voltage Network.....32

3.7 The Mixer.....33

3.8 The Amplifier and the First Filter.....35

3.9 The Swept-Gain Stage.....36

3.10 The AGC Signal Network.....37

3.11 The Resolution Filter.....38

3.12 The Detector.....39

3.13 The Post Amplifier.....41

**4.0 RESULTS.....42**

4.1 Dynamic Range Test.....42

4.2 Frequency Calibration.....43

4.3 Probing Experiments and Results.....45

**5.0 CONCLUSION AND RECOMMENDATIONS.....51**

**REFERENCES.....53**



Classification For

GROUP CLASS

SECRET

Unclassified

Classification

---

Distribution/

Availability Codes

Avail and/or

Special

A1

## LIST OF FIGURES

FIGURE 1:	Instantaneous Frequencies for Point Target with Delay T.....	3
FIGURE 2:	Instantaneous Frequency of Output.....	3
FIGURE 4:	Expanded View of Part of Sweep.....	5
FIGURE 5:	Spectrum of Received and Transmitted Signal.....	6
FIGURE 6:	Amplitude Spectrum of a Point Target Located 4 m from the Antenna.....	7
FIGURE 7:	Amplitude Spectrum of a Point Target Located 4 m from the Antenna.....	8
FIGURE 8:	Amplitude Spectrum of a Point Target Located 4 m from the Antenna.....	9
FIGURE 9a:	Scanning Spectrum Analyzer.....	13
FIGURE 9b:	Shifting of the Input Signal and Passing It Through the Filter.....	14
FIGURE 10:	Resolution Constraint.....	16
FIGURE 11:	Filter Response of a Point Target Located 4 m from the Antenna.....	17
FIGURE 12:	Filter Response of a Point Target Located 4 m from the Antenna.....	18
FIGURE 13:	Filter Response of a Point Target Located 4 m from the Antenna.....	19
FIGURE 14:	Block Diagram of the Spectrum Analyzer.....	20
FIGURE 15a:	Pre-Amplifier Circuit.....	24
FIGURE 15b:	Reflection of Base Into Emitter.....	25
FIGURE 15c:	Small Signal Circuit of Pre-Amp.....	26
FIGURE 16:	The Voltage-Controlled Oscillator Circuit.....	27
FIGURE 17a:	The Sweep Generator Circuit.....	29
FIGURE 17b:	Output of the Timer for Single Sweep.....	31
FIGURE 17c:	Output of the Timer for Continuous Sweep.....	31
FIGURE 17d:	Output of the One Shot (74121) for Continuous Sweep.....	31
FIGURE 17e:	The Ramp Generator Output.....	32
FIGURE 18:	The Sweep Network for VCO.....	33
FIGURE 19:	The Mixer Circuit.....	34
FIGURE 20:	Gain Characteristics of the Mixer (MC1496).....	34
FIGURE 21:	The Amplifier, Filter and Buffer.....	35
FIGURE 22a:	Wide Band Amp. Response.....	36

FIGURE 22b: The Wideband Amplifier (Swept Gain Stage).....	37
FIGURE 23: The Sweep Network for AGC.....	38
FIGURE 24: The Circuit of the Resolution Filter.....	39
FIGURE 25: The Detector Circuit.....	40
FIGURE 26: The Post Amplifier.....	41
FIGURE 27: Spectrum Analyzer Response.....	43
FIGURE 28: Frequency Calibration Curve.....	44
FIGURE 29a: Delay Line Return (by the HP3585A Spectrum Analyzer).....	45
FIGURE 29b: Delay Line Return (by the Spectrum Analyzer).....	46
FIGURE 30a: Ground Return (by the HP3585A Spectrum Analyzer.....	46
FIGURE 30b: Ground Return (by the Spectrum Analyzer).....	47
FIGURE 31a: Bottom of the Bucket and the Ground Returns (by the HP3585A Spectrum Analyzer).....	47
FIGURE 31b: Bottom of the Bucket and the Ground Returns (by the Spectrum Analyzer).....	48
FIGURE 32a: Concrete and Metal Returns (by the HP3585A Spectrum Analyzer).....	48
FIGURE 32b: Concrete and Ground Returns (by the Spectrum Analyzer).....	49
FIGURE 33a: Concrete and Metal Plate Returns (by the HP3585A Spectrum Analyzer).....	49
FIGURE 33b: Concrete and Metal Plate Returns (by the Spectrum Analyzer).....	50
FIGURE 34: The Experiment Set-Up Showing the Bucket and Antenna.....	50
FIGURE 35: The Experiment Set-Up Showing the Bucket and the Concrete and the Antenna.....	51

## ABSTRACT

↓ A spectrum analyzer is required for analyzing the signal received by an FM-CW radar. For probing the ground and sea ice with an FM radar, logistics and economics considerations limit the kind of spectrum analyzer used. These limitations suggest the need for a simple, yet adequate and portable, spectrum analyzer. Hence, a spectrum analyzer was specified, designed and developed to serve these purposes. This report briefly introduces the kind of radar used for these probing experiments and extensively describes the design and performance of this special-purpose spectrum analyzer. ↗

### 1.0 INTRODUCTION

In recent years, the ability to detect thickness of sea ice and identification of layers within temperate glaciers [1,2], location of metallic and plastic gas and water pipes [3-5], presence and thickness of stratified media [6], detection of voids in concrete [7] and archaeological mapping [8] has focused a greater attention on the field of probing. Most of the studies on shallow probing have used impulse radars [2,9-11]. Frequency-modulated continuous-wave (FM-CW) radars have been investigated and proven to have advantages over the impulse radars.

The theoretical concept of FM-CW radar is introduced in the early sections of this report. The spectrum evaluation, corresponding filter responses, resolution constraints and other parameters regarding the analysis of the returned signal spectrum are then discussed. These parameters and constraints are shown to be the determining factors in the design of the spectrum analyzer. The later sections of the report deal with the detailed

design procedures, and circuit diagrams are presented along with the spectrum produced by several known signals. The dynamic range of the analyzer is discussed, and suggestions are made for future modifications.

### 1.1 The FM-CW Radar

The major use of CW radar is to measure the relative velocity of a moving target. Due to the relatively narrow bandwidth of the transmitted signal in this system, unambiguous range measurement is impossible. To measure range unambiguously, there must be some distinction between the time of transmission and reception of the carrier. Modulation can provide timing marks on the carrier by which this time could be measured. To measure the range more accurately, these timing marks must be sharper. This means the bandwidth of the transmitted signal must increase [12].

Various modulation schemes could be used to broaden the spectrum of a radar. Amplitude modulation is used in pulse radars; the shorter the pulse, the more accurate the range measurement [12]. Frequency-modulation (FM) is another widely used technique. An FM radar altimeter was first introduced in 1939 [13]. In this technique, the timing is achieved by rapid changing of the frequency.

Figure 1 illustrates the instantaneous frequencies of transmitted and received signals for an FM radar observing a point target. During a time interval  $T_R/2$  sec, the transmitted signal is linearly swept over a bandwidth,  $B$ . During the next  $T_R/2$  sec interval it is linearly swept back to the original frequency. Hence, the bandwidth of the signal is the difference between the two extreme frequencies between which the carrier is swept; that is, the bandwidth  $B$  is  $f_2 - f_1$ (Hz). The received signal is a replica of the transmitted signal delayed by a time  $T$ . Due to the travel time of the signal

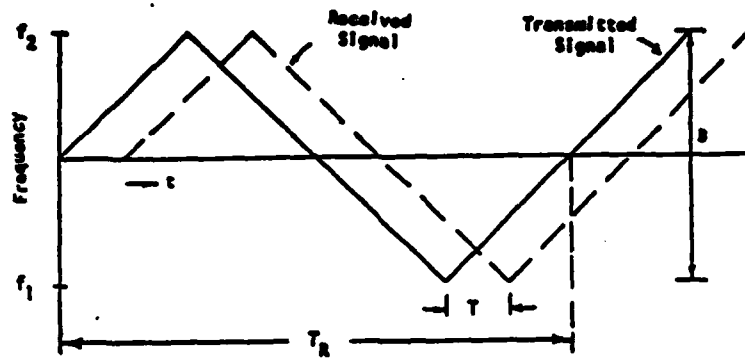


FIGURE 1: Instantaneous Frequencies for Point Target with Delay T

to the target and back,  $T$  is  $2R/c$  sec ( $R$  is the range of target in meters and  $c$  is the speed of light in m/sec). At each point in time, the difference between the frequencies of the transmitted and received signal is directly related to this time delay  $T$ . This instantaneous frequency difference is shown in Figure 2. Instead of using a triangle wave to modulate the frequency, other periodic waveforms such as sawtooth or sine wave can also be used.

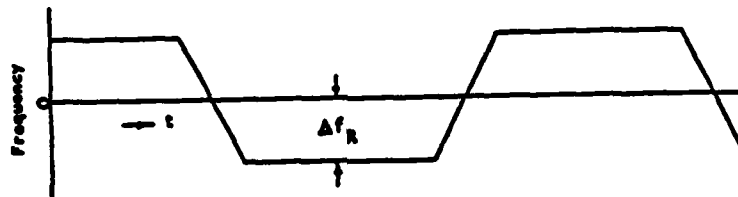


FIGURE 2: Instantaneous Frequency of Output

The basic components of a simple FM homodyne radar are shown in Figure 3. The carrier frequency is modulated by a triangle waveform. This modulated signal is transmitted via the transmitting antenna, while a portion of it is coupled into a mixer. The transmitted signal goes out to the target and its echo is received by the receiving antenna. This signal is then mixed with the

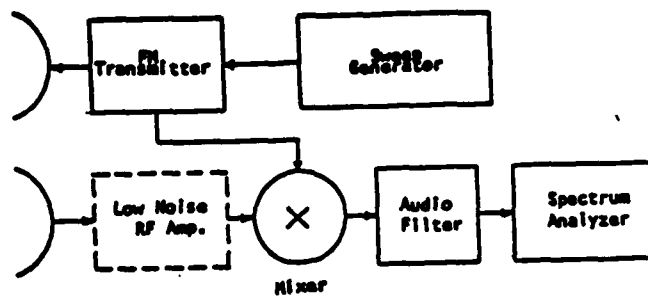


FIGURE 3: Simple FM Radar

- coupled transmitted signal. The output of the mixer is then filtered so that the frequency difference component of these two signals,  $\Delta f$ , is recovered. A frequency meter or a spectrum analyzer is used to display the results.

### 1.2 FM-CW vs Impulse Radar

An FM radar has several advantages over an impulse radar for probing into lossy media. A wide bandwidth is associated with a relatively short video-pulse. An impulse radar transmitting these short video-pulses requires an antenna with characteristics that remain constant over a wide band of frequencies. This is not an easy task to accomplish. Therefore, the result is that most video-pulse radars produce outputs from point targets that ring like a damped sine wave. This problem is further complicated by the receiving antenna which converts an impulse into a double impulse. In FM radars, on the other hand, the correction for varying antenna properties can be inserted before transmission via feedback from the received signal to control the amplitude of the transmitter output. In turn, the signal received through a non-distorting path is constant over the bandwidth [14].

Impulse radars operate with high powers and their components should be specified accordingly. For an FM system the peak and average power of the

signal are the same. This feature permits implementation of the system using low-power, low-voltage, solid-state components.

### 1.3 Location of Target Response in Frequency Spectrum

The relationship between the time delay  $T$  and  $\Delta f$  is shown in Figure 4 to be:

$$\Delta f = \frac{df}{dt} T$$

From Figure 1 we get

$$\frac{df}{dt} = \frac{2B}{T_R}$$

Hence:

$$\Delta f = \frac{2BT}{T_R}$$

and we know  $T = 2R/c$ , therefore:

$$\Delta f = \frac{4BR}{cT_R} \quad (1)$$

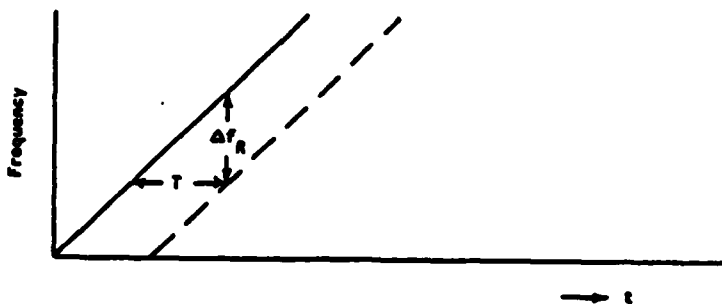


FIGURE 4: Expanded View of Part of Sweep

This is true when the medium is air. For lossy media with greater dielectric constant than air, equation (1) must be multiplied by  $\sqrt{\epsilon_m}$ , where  $\epsilon_m$  is the dielectric constant of the medium. Thus, the value of  $\Delta f$  is directly related to the target distance. Figure 5 shows the spectrum of the transmitted signal and the filtered output signal.

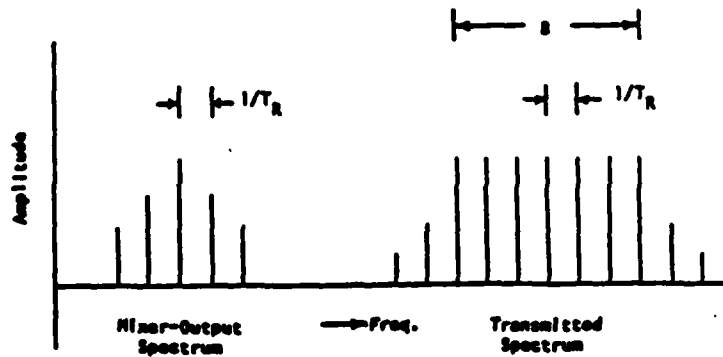


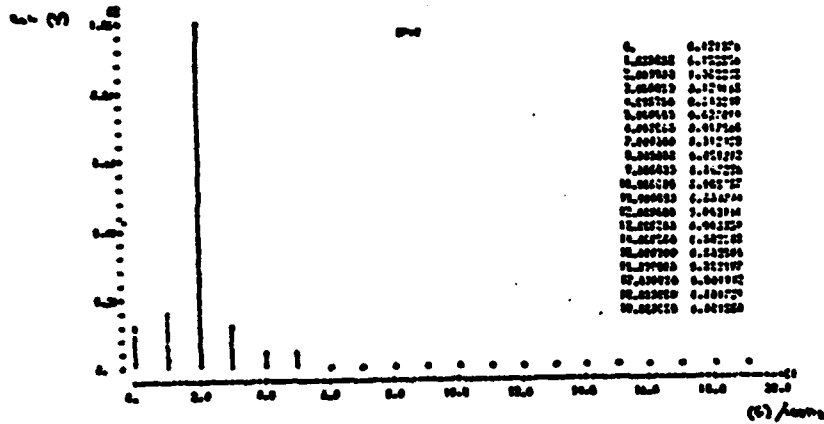
FIGURE 5: Spectrum of Received and Transmitted Signal

If the carrier is linearly swept in one direction, the spectrum of the filtered mixer output will consist of one component at  $\Delta f$ . Because the FM waveform is periodic, the filter output is maximum near  $\Delta f$ , but consists of a series of harmonics of the sweep repetition rate  $1/T_R$ . As seen in equation (1), any change in the value of  $T_R$  will cause a change in the location of the peak of the filter output spectrum and therefore the relative strength of the harmonics.

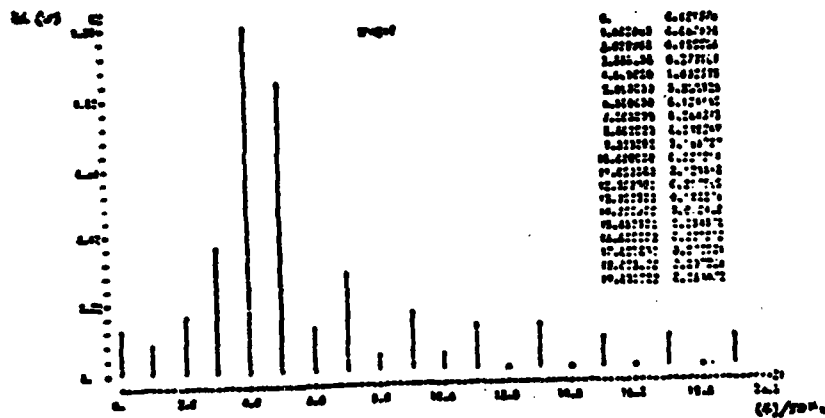
It is shown [15] that the finite Fourier transform of the mixer is:

$$V_{IF} = \frac{\sin(\omega_a - \omega)T_R/2}{\omega_a - \omega} + \frac{\sin(\omega_a + \omega)T_R/2}{\omega_a + \omega}$$

where  $\omega_a = 2\pi aT$  with  $a$  = rate of change of frequency. This is the only output because the filter only passes the difference of the two frequencies and rejects the sum. The effects of various FM rates on the amplitudes of the harmonics of  $1/T_R$  are shown in Figures 6-8 [15].



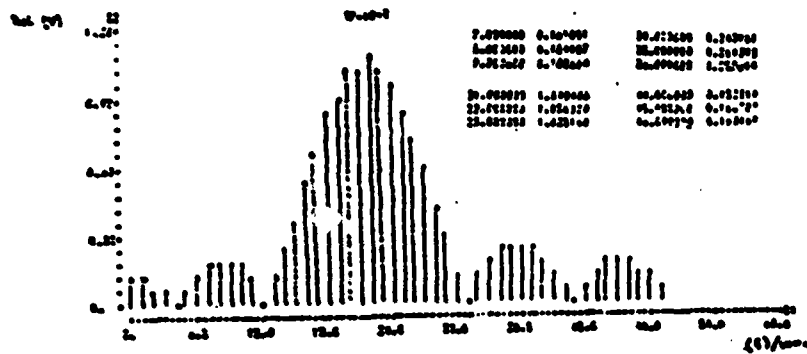
(a)



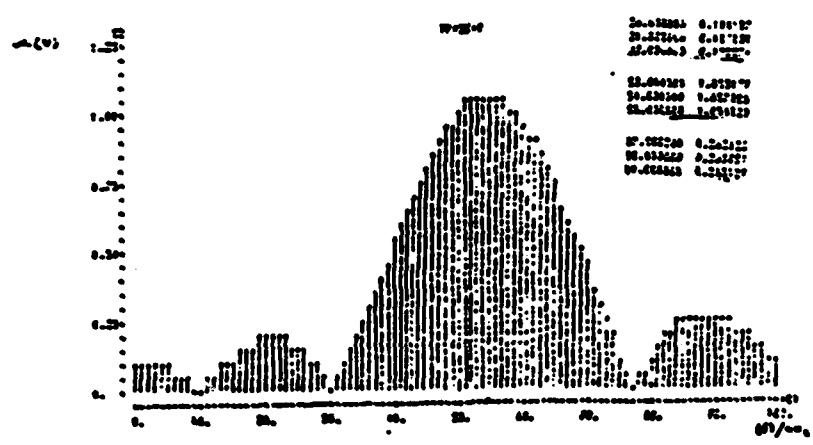
(b)

FIGURE 6: Amplitude Spectrum of a Point Target Located 4 m from the Antenna. (a) PRF = 100 Hz; (b) PRF = 50 Hz





(a)



(b)

FIGURE 8: Amplitude Spectrum of a Point Target Located 4 m from the Antenna. (f) PRF = 10 Hz; (g) PRF = 4 Hz

1.4 Penetration Depth

The electric field associated with a wave propagating in the direction z, normal to the interface of a medium, can be represented by:

$$E_x = E e^{-jkz} \tag{2}$$

where:

E = the electric field at the interface.

k = the wave number given by

$$k = \omega \sqrt{\mu \epsilon_c}$$

Here  $\epsilon_c$  is the complex permittivity given by

$$\epsilon_c = \epsilon' - j\epsilon''$$

and  $\mu$  is the permeability of the medium. Thus, we can write:

$$k = \omega \sqrt{\mu(\epsilon' - j\epsilon'')}$$

This can be written as

$$jk = \alpha + j\beta = j\omega \sqrt{\mu\epsilon' (1 - j(\epsilon''/\epsilon'))}$$

where  $\alpha$  is the attenuation constant and  $\beta$  is the phase constant. Thus, equation (2) can be written as

$$e^{-jkz} = e^{-\alpha z} e^{-j\beta z} \quad (2a)$$

The first factor shows the attenuation of a wave that propagates through a medium. This attenuation is a function of the frequency and the dielectric properties of the medium. The ratio  $\epsilon''/\epsilon'$  is called the loss tangent of the medium ( $\tan\delta$ ). The expressions for  $\alpha$  and  $\beta$  can be expressed as:

$$\alpha = k_0 \left[ \left( \sqrt{1 + \tan^2\delta} - 1 \right) / 2 \right]^{1/2}$$

and

$$\beta = k_0 \left[ \left( \sqrt{1 + \tan^2\delta} + 1 \right) / 2 \right]^{1/2}$$

where  $k_0 = \omega \sqrt{\mu\epsilon'/2}$ .

## 2.0 SPECTRAL MEASUREMENTS AND SPECTRUM ANALYSIS

As discussed in the previous section, there is a direct relationship between the relative location (range) of a target and the output frequency content of an FM radar. Thus, a spectral study of the radar output signal is needed. A simple and commonly used method to obtain the spectrum is to use an analog spectrum analyzer to determine the spectral density of the radar output signal.

### 2.1 Scanning Spectrum Analyzer

The power spectral density of a signal  $x(t)$  at frequency  $f_c$  may be obtained by passing  $x(t)$  through a narrow bandpass filter centered at  $f_c$  with a bandwidth of  $B_s$  and detecting the output. The average power out of a filter with  $B_s$  is less than the detailed character of the input spectrum.

$$S_{out} = \lim_{T \rightarrow \infty} \frac{1}{T} \int_{-T/2}^{T/2} |y(t)|^2 dt$$

by Parseval's theorem we have

$$\int_{-\infty}^{\infty} |x(t)|^2 dt = \int_{-\infty}^{\infty} |X(f)|^2 df$$

also, we know that

$$G_x(f) = \lim_{T \rightarrow \infty} \frac{1}{T} |X(f)|^2$$

thus, by assuming a narrow bandpass filter we get

$$S_{out} = \lim_{T \rightarrow \infty} \frac{K^2}{T} \left[ \int_{-f_c - B_s/2}^{f_c + B_s/2} |X(f_c)|^2 df + \int_{-f_c - B_s/2}^{f_c + B_s/2} |X(f_c)|^2 df \right]$$

$$= \lim_{T \rightarrow \infty} \frac{K^2}{T} [ |X(-f_c)|^2 B_s + |X(f_c)|^2 B_s ]$$

$$X(-f_c) = X(f_c),$$

so

$$S_{out} = \lim_{T \rightarrow \infty} \frac{K^2}{T} 2B_s |X(f_c)|^2$$

or

$$S_{out} = 2K^2 B_s G_x(f_c)$$

where  $G_x(f_c)$  is the power spectral density of the input  $x(t)$  at  $f_c$  and  $K^2$  is the filter power gain. If  $K^2 = 1/2 B_s$ , then

$$S_{out} = G_x(f_c)$$

This average output power value can be measured by passing the filter output through a square-law device and an integrator. Thus, to measure the spectral power density of a signal at various frequencies, filters centered at the respective frequencies are needed.

To measure the power spectral density of a signal across a known frequency band, a sweeping, or scanning, spectrum analyzer may be used. This spectrum analyzer uses an electronically tuneable bandpass filter which scans across the desired frequency band. The same results can be obtained by a system for which the center frequency of the filter is fixed, but the input signal spectrum is swept into the passband of the filter by frequency translation. This frequency translation (modulation) is done by multiplying the

input signal by a periodic waveform whose frequency is slowly changing. Figure 9(a) shows the diagram of such a spectrum analyzer.

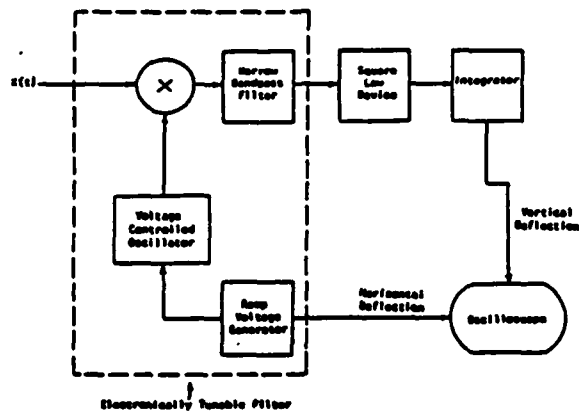
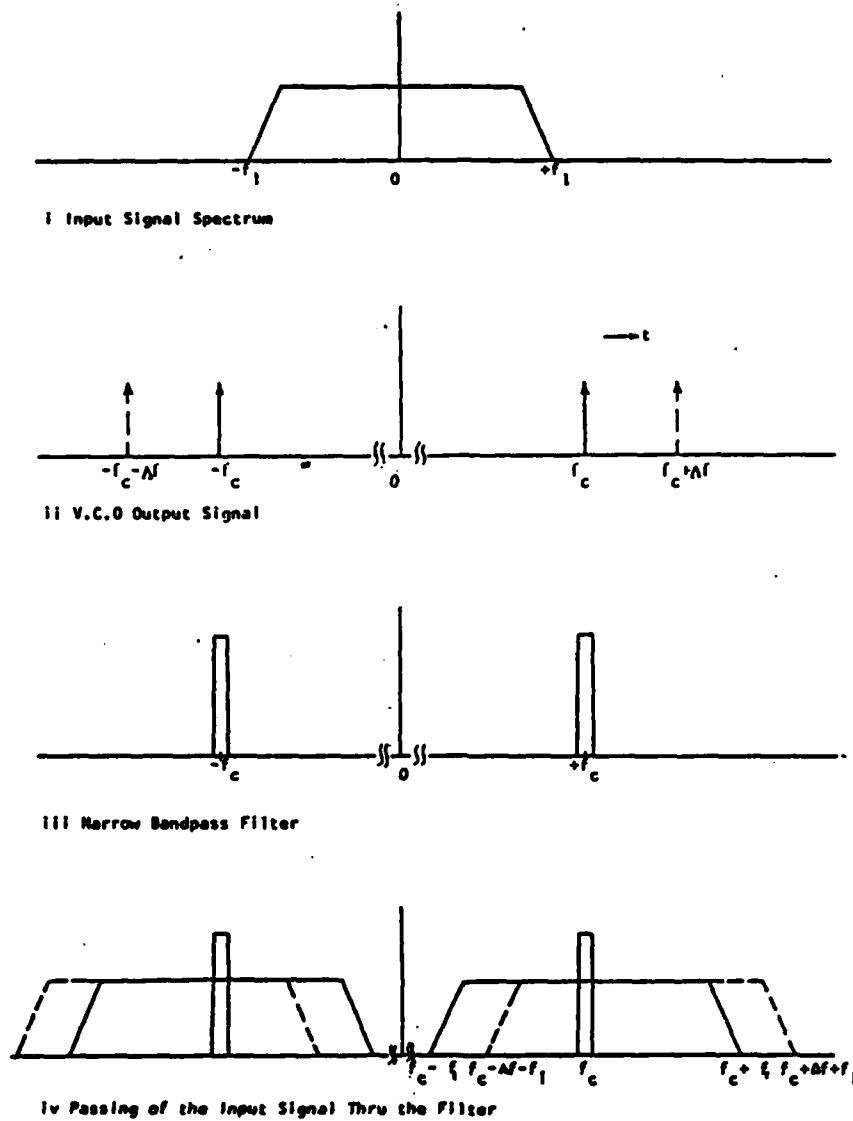


FIGURE 9a: Scanning Spectrum Analyzer

This slowly changing frequency is usually produced by a voltage controlled oscillator (VCO). A ramp voltage generator is needed to control the VCO. The oscillator signal is then multiplied by the input signal  $x(t)$  which causes the spectrum of  $x(t)$  to shift by the amount of the VCO frequency. As the ramp voltage increases, the VCO frequency increases. The result is the passing of the input signal spectrum through the passband of the filter. Suppose that the filter is centered at  $f_0$  and the VCO output signal starts from  $f_0$  and slowly increases to  $f_1$  during one sweep. At any point of time during the sweep the VCO output signal is  $f_0 + \Delta f$  and, as the input signal component at  $\Delta f$  gets multiplied by the VCO output, it will be shifted to  $f_0 + 2\Delta f$  and  $f_0$ . The component at  $f_0 + 2\Delta f$  is rejected by the filter and the component at  $f_0$  passes through the filter. Therefore, as  $\Delta f$  increases by time, the corresponding input signal component will be passed through the filter. This is illustrated in Figure 9(b).



**FIGURE 9b: Shifting of the Input Signal and Passing It Through the Filter**

The ramp voltage can be used as the x input of an x-y recorder or the horizontal input of an oscilloscope. The output of the detector-integrator (proportional to the power spectral density of  $x(t)$ ) is used as the y input of an x-y recorder or the vertical input of an oscilloscope. This way a display of  $G_x(f)$  vs frequency is produced [16].

## 2.2 Filter Bandwidth and Resolution

Several constraints affect the choice of system parameters. The accuracy of a spectrum analyzer is improved by a slower ramp sweep rate and narrower filter bandwidth. Both of these will increase the time during which the spectrum of a signal is produced. For a good design criterion it is shown [17] that the time required to sweep past the filter should be at least 2.3 times the reciprocal of the filter bandwidth. Hence the narrower the filter bandwidth, the longer time required to sweep the signal past it. Also, it is clear that for longer sweep time, a longer time is spent on producing the spectrum of a signal.

If the sweep rate is  $\Delta f/\Delta t$  and the filter bandwidth is  $B_s$  Hz, then the sweep goes through  $B_s$  (Hz) in  $\Delta f/\Delta t$  seconds. If the filter rise time is  $t_R$  and of the order of  $1/B_s$  seconds, then for the filter to achieve a nearly steady-state response we must have:

$$\frac{B_s}{\Delta f/\Delta t} > \frac{1}{B_s} \quad \text{or} \quad \frac{\Delta f}{\Delta t} < B_s^2$$

which means the rate of the frequency change (Hz/sec) must not be greater than  $B_s^2$  (Hz/sec).

The finite filter bandwidth limits the resolution of the spectrum analyzer. This limitation is shown in Figure 10. If the filter bandwidth is greater than the spacing between spectral lines, two or more spectral lines will fall in the passband of the filter, so individual lines cannot be resolved by the spectrum analyzer.

When we look at a target, there is a range and a respective IF spectrum associated with it. For very narrow filter bandwidth (centered at the IF spectral lines), if the  $f_{IF}$  associated with the target is an integer multiple of the  $f_m$  rate (i.e.,  $f_{IF} = n f_m$ ,  $n = 1, 2, \dots$ ) then the target falls right on

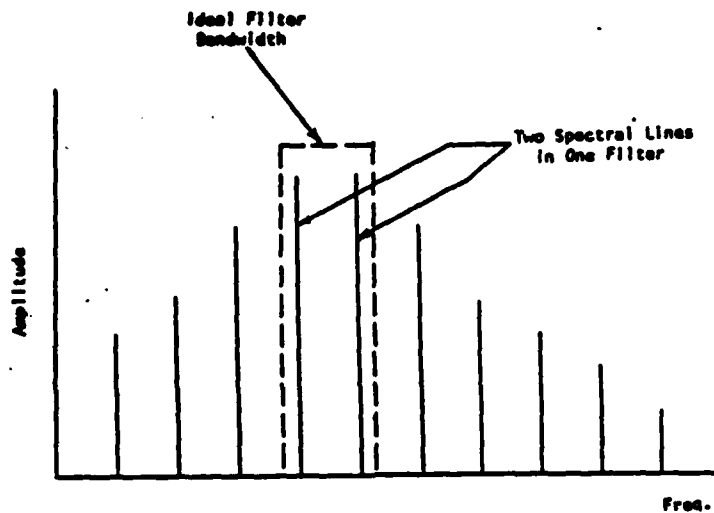
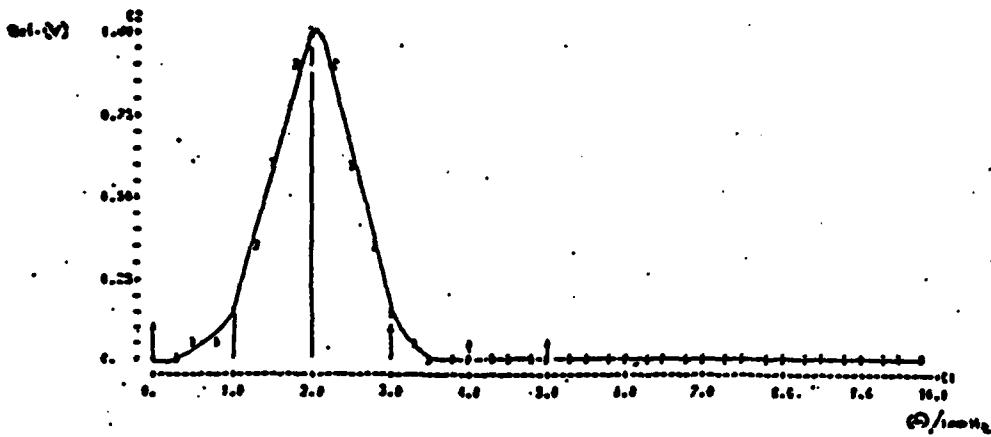


FIGURE 10: Resolution Constraint

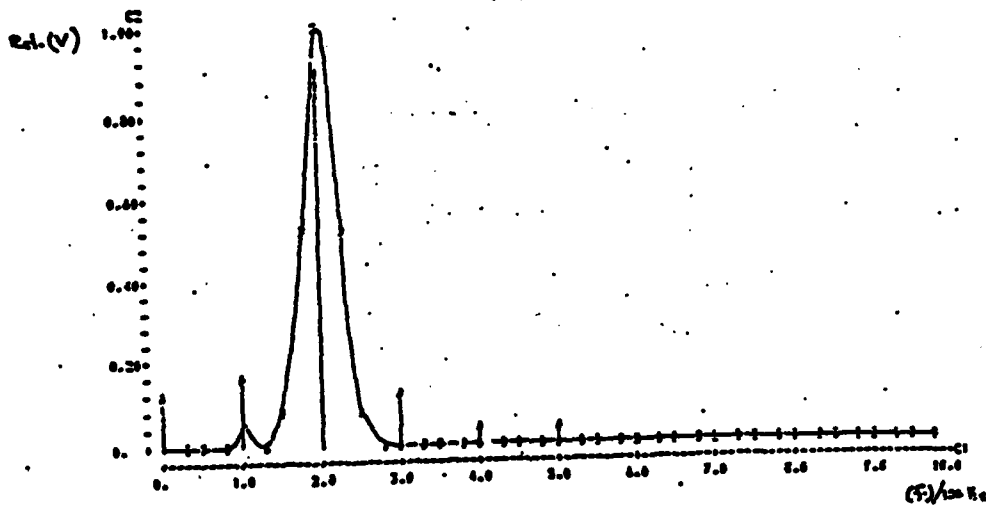
the spectral lines and can correctly be located. But, if the  $f_{IF}$  is not an integer multiple of the fm rate (i.e.,  $f_{IF} = 2.6 \text{ fm}$ ) which means that the target falls between the spectral lines, then its location cannot be recognized correctly. If the filter bandwidth is too wide and two or more closely located targets fall within its passband, they cannot be individually distinguished. This reduces the resolution of the system.

The combined effects of spectrum analyzer filter bandwidth and radar pulse repetition frequency for a target 4 m away from the antenna are shown in Figures 11-13 [15]. These figures clearly show that the optimum interpretability is obtained when the filter bandwidth is equal to or slightly greater than the radar pulse repetition frequency [15].

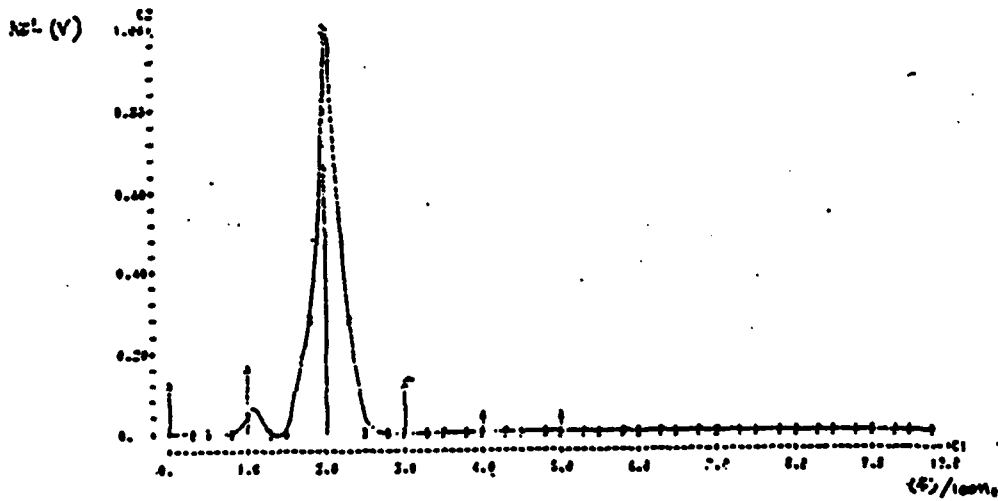
There are many types of spectrum analyzers on the market today, from very simple to those capable of analyzing spectra from 20 Hz to 40 MHz and higher with variable resolution down to 3 Hz. The more sophisticated they get, the more expensive they become. Therefore, to maintain reasonable cost and size for a specific purpose, one must sacrifice some of the flexibility of these



(a)

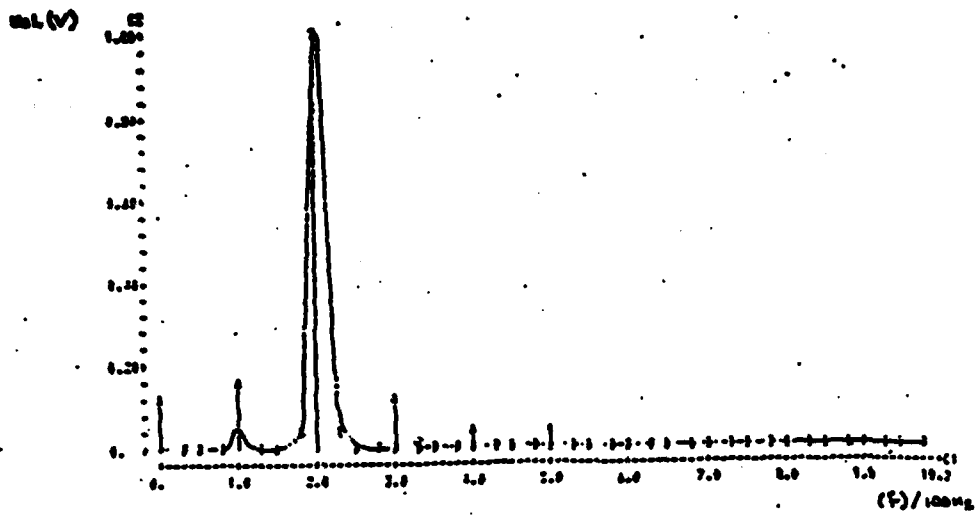


(b)

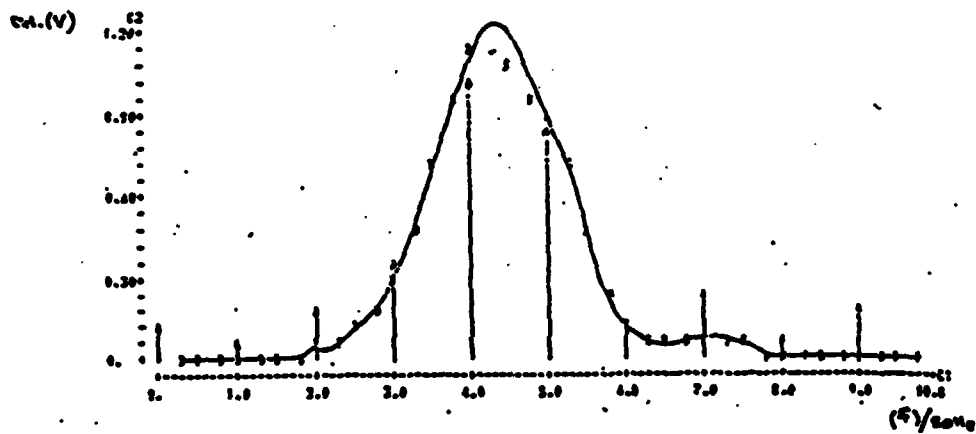


(c)

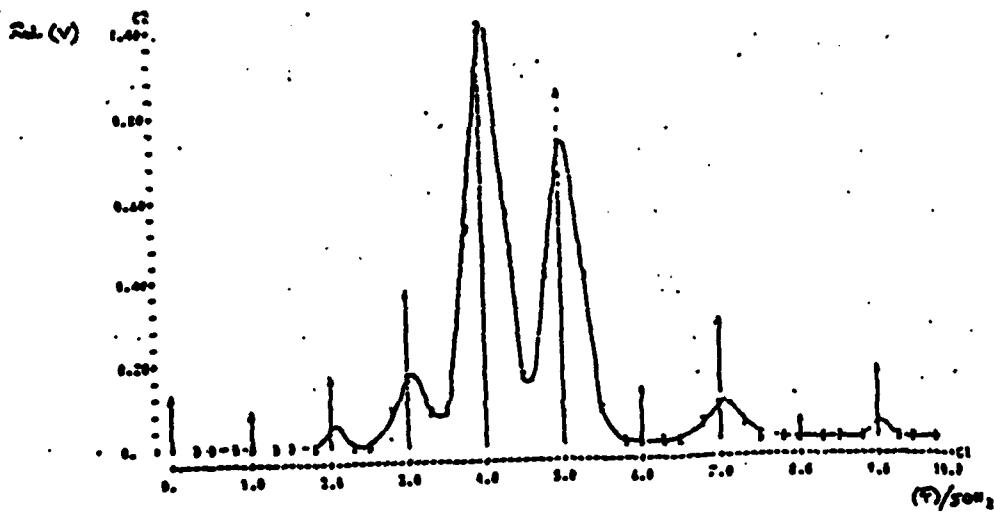
FIGURE 11: Filter Response of a Point Target Located 4 m from the Antenna  
 PRF = 100 Hz. Filter Bandwidth = (a) 100 Hz; (b) 45 Hz, (c) 32 Hz



(a)

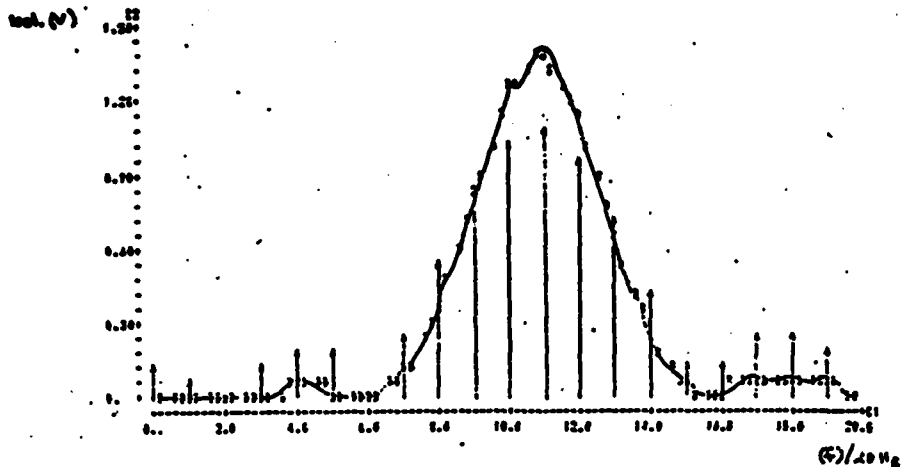


(b)

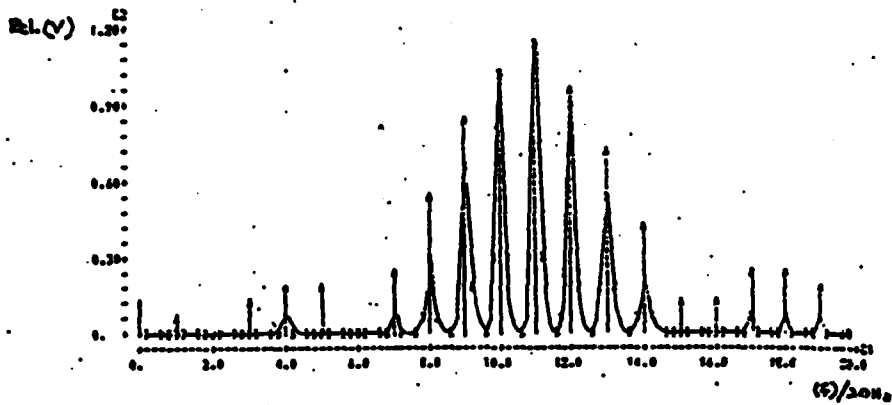


(c)

FIGURE 12: Filter Response of a Point Target Located 4 m from the Antenna.  
 (a) PRF = 100 Hz, Filter Bandwidth = 20 Hz; (b) PRF = 50 Hz, Filter Bandwidth = 50 Hz; (c) PRF = 50 Hz, Filter Bandwidth = 22.5 Hz



(a)



(b)

FIGURE 13: Filter Response of a Point Target Located 4 m from the Antenna. PRF = 20 Hz. Filter Bandwidth = (a) 20 Hz, (b) 6 Hz

general-purpose analyzers. Thus, other constraints on the resolution of the spectrum analyzer are cost and size.

### 3.0 SPECTRUM ANALYZER DESIGN

The concepts of an FM-CW radar, the signal spectrum, and the scanning spectrum analyzer have been introduced up to this point. The rest of this report focuses on the detailed design of a spectrum analyzer.

#### 3.1 Description of the Spectrum Analyzer

The block diagram of the spectrum analyzer is shown in Figure 14. The input signal, which is provided by the IF output of the radar, is amplified and then fed to the mixer (modulator). A sweep generator produces the appropriate frequencies through the voltage-controlled oscillator (VCO) whose output is also fed to the mixer. The output of the mixer is then amplified and passed through a bandpass filter to remove the unwanted noise from the signal. The output of this filter is fed through a buffer to a wideband amplifier whose gain is controlled by an "AGC" input. The necessary signal for this "AGC" input is provided by the sweep generator. The reason for using a swept-gain amplifier is presented later. The output of this amplifier is applied to a 200-Hz-wide bandpass filter (resolution filter). The output of

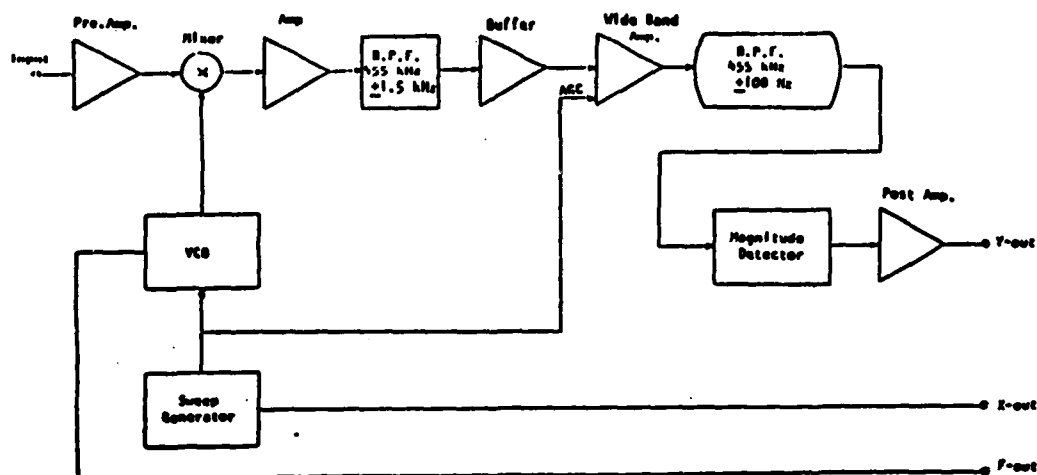


FIGURE 14: Block Diagram of the Spectrum Analyzer

the resolution filter is applied to a magnitude detector and finally to an amplifier whose output is the output of the spectrum analyzer. This signal, along with a sample of the sweep generator output, can be used to deflect the y and x inputs of an x-y recorder or the vertical and horizontal channels of an oscilloscope. A frequency output from the VCO is also provided so that, by using a frequency meter, the output of the VCO can always be monitored. If this output is to be used for the digital recording of the frequency vs y-output, a frequency-to-voltage conversion is required. The following sections describe the functions and circuit design of each block.

### **3.2 Parameter Selections and Design Considerations**

Parameters and the design considerations must be known prior to the design procedure. As the building and the design advances, some of these parameters and considerations may change. In this case, as the design advanced, some of the parameters were changed due to cost and time constraints. The choice of parameters such as resolution bandwidth, sweep rate gain, etc. are discussed here.

#### **3.2.1 Resolution Bandwidth**

A narrow BPF was required for this system. A BPF with 200 Hz resolution bandwidth and centered at 455 kHz was already available in the laboratory. Two-hundred Hz is narrow enough, and parts that operate at 455 kHz are readily obtained. Hence, due to the cost considerations, this BPF was to be used as the resolution filter (several months later it was discovered that this filter didn't have a nice frequency response in its passband region, so a better filter with the same parameters was bought).

### 3.2.2 Sweep Rate

In Section 2.2, the relationship between the sweep rate ( $\Delta f/\Delta t$ ) and the resolution bandwidth ( $B_g$ ) was discussed. It was also explained that it is desirable to have longer sweep times. Sweep times of 15 and 30 seconds (for both single- and continuous-sweep modes) were chosen; both of these times satisfy the theoretical requirements.

### 3.2.3 Gain Between Stages

A spectrum analyzer should have a large dynamic range. The level of radar return signals from our systems usually varies between -100 dBm and -10 dBm. Hence, the spectrum analyzer should be able to detect signal levels in this range. By virtue of the design, the mixer has a gain of 12 dB and the total loss through the filters is 8 dB. The detector does not properly detect signal levels lower than -38 dBm. For the low-level signals, the total gain from the input of the spectrum analyzer to the input of the detector must be:

$$-100 + \text{total gain (dB)} + 12 - 8 > -38 \text{ dBm}$$

so, total gain  $> 58$  dB. This gain should be distributed before and after the mixer. Hence, a preamplifier with 20 dB gain was decided upon. Hence, additional gain of 38 dB is required between the mixer and the detector. High level signals would be saturated by going through these amplifiers. Hence, at this stage a log amplifier or a swept-gain amplifier should be used. At 455 kHz, a gain-controlled amplifier is easier to build than a log amplifier. This swept-gain amplifier attenuates the high-level signals and amplifies the low-level signals. An amplifier with 23.5 dB gain is put between the mixer and the first filter and the swept gain amplifier is put between the two filters. Depending on the gain or loss at the swept-gain stage, it was estimated

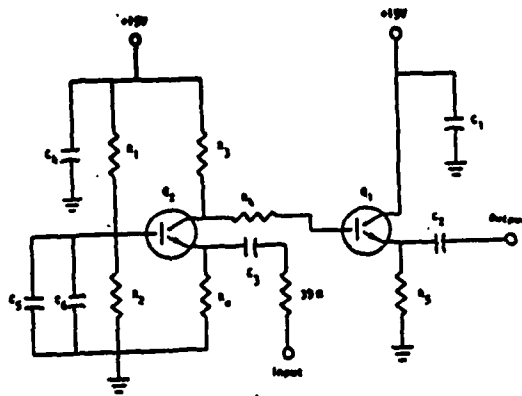
and verified that a post amplifier with 40 dB gain (after the detector) could produce output signal levels from 300 mV up to 5 volts -- a suitable voltage range for x-y recorder and A/D converter used in digital recorders.

### 3.2.4 Construction Considerations

A spectrum analyzer deals with low-level signals, so it is important to avoid any noise problems and unwanted coupling of signals from one circuit to another. It was decided to have one circuit board for the power supply circuits, one for the mixer and VCO, another for the filters, swept-gain stage and detector, and one for the pre- and post-amplifiers along with the ramp generator circuit. To avoid ground loops, the ground leads from all the boards are brought together to the VCO board and are connected to the VCO ground. Heavy wires are used for ground connections. All the boards are properly shielded. Through testing it was discovered that the center tapped lead of the transformer created a ground loop with considerable noise. Therefore, the center-tapped lead was left floating and the problem was eliminated. The chassis was properly grounded. All the supply voltages were properly filtered before connecting to a chip or transistor.

### 3.3 Pre-Amplifier

An amplifier with 20 dB gain and low input impedance is needed as the preamplifier. The IF output of the radar has an impedance of 50 ohms. Hence, a common-base amplifier was used for this purpose. Furthermore, we require 2 volts rms clipping which means maximum voltage at the emitter should not exceed 2 volts (this amplifier was placed before the resolution filter in the earlier design and 2 volt rms voltage was required to protect the filter).



$R_1 = 8.2 \text{ K ohms}$   
 $R_2 = 1.5 \text{ K ohms}$   
 $R_3 = 560 \text{ ohms}$   
 $R_4 = 1.0 \text{ K ohms}$   
 $R_E = 100 \text{ ohms}$   
 $R_E = 100 \text{ ohms}$   
 $C_1 = C_2 = C_3 = 0.01 \mu\text{F}$   
 $C_1 = 47 \mu\text{F}$   
 $C_2 = 47 \mu\text{F}$   
 $Q_1 = \text{MPS Darlington}$   
 $Q_2 = \text{LT1001A}$

FIGURE 15a: Pre-Amplifier Circuit

Figure 15a shows the circuit of this amplifier. The small signal analysis of this circuit is as follows:

$$\text{Gain} = 20 \text{ dB}$$

$$h_{fe} = 70 \text{ (typical)}$$

$$h_{oe} = 10^{-4} \text{ sec}$$

$$V_{EE} = 2 \text{ V}$$

$$V_{BB} = 2 + .7 = 2.7 \text{ V}$$

$$V_{BB} = \frac{R_2}{R_1 + R_2} (15)$$

$$R_1 = 4.56 R_2$$

$$\text{Choose } R_1 = 8.2 \text{ K ohms}$$

$$\text{hence, } R_2 = 1.8 \text{ K ohms}$$

$$\text{Choose } R_2 = 1.5 \text{ K ohms}$$

So actually

$$V_{bb} = \frac{1.5}{8.2 + 1.5} (15) = 2.32 \text{ V}$$

$$R_b = 1.5 \parallel 8.2 = 1.27 \text{ K ohms}$$

This resistance is reflected into the emitter circuit as:

$$R_b / (h_{fe} + 1) = 17.88 \text{ ohms}$$

From Figure 15b we calculate  $I_{EQ}$ :

$$I_{EQ} = \frac{2.32 - .7}{17.88 + R_e} = \frac{1.62}{17.88 + R_e} \quad (1)$$

$$h_{ie} = V_T h_{fe} / I_{EQ} \quad , \quad V_T = 25 \text{ mV}$$

hence:

$$h_{ie} = 1.75 / I_{EQ} \text{ ohms}$$

$$h_{fb} = h_{fe} / h_{fe} + 1 = -.99$$

$$h_{ib} = h_{ie} / h_{fe} + = 24.6 / I_{EQ} \text{ K ohms} \quad (11)$$

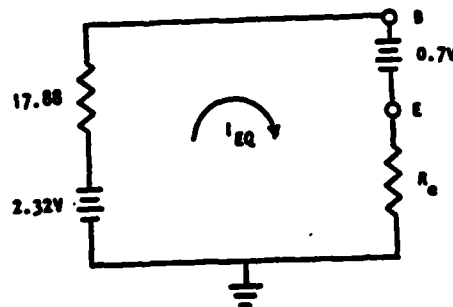


FIGURE 15b: Reflection of Base Into Emitter

### Current Gain

For common-base amplifier the current gain is slightly less than 1, so:

$$A_i = .9$$

From Figure 15c, we get:

$$h_{fb} i_e = -.99 i_e$$

$$1/h_{ob} = (h_{fe} + 1)/h_{oe} = 710 \text{ K ohms}$$

$$A_i = .9 = i_e i_c i_L / i_j i_e i_c = 50/50 + h_{ib} (.99) = 710/710 + .56$$

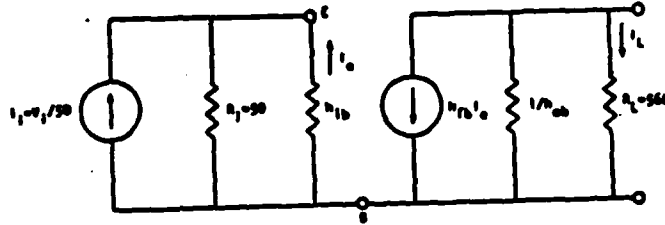


FIGURE 15c: Small Signal Circuit of Pre-Amp

Hence:

$$h_{ib} = 4.96$$

From (11) we get:

$$I_{EQ} = 4.96 \text{ mA}$$

$$h_{ie} = 352.82 \text{ ohms}$$

From (1) we get:

$$R_e = 140.51 \text{ ohms; choose } R_e = 120 \text{ ohms.}$$

### Voltage Gain

$$A_v = V_L / V_i = V_L i_e / i_e V_i$$

$$i_e = \left( \frac{V_i}{50} \right) \left( \frac{-50}{50 + 4.96} \right) = V_i / 54.96$$

$$V_L = -.99 i_e (560) = -554.4 i_e$$

$$A_v = -554.4 / -54.96 = 10.09 \text{ or } 20.08 \text{ dB}$$

The output is then applied to the mixer signal input via a buffer ( $O_1$ ) shown in Figure 15a.

### 3.4 Voltage-Controlled Oscillator

As explained earlier, the voltage-controlled oscillator starts at a frequency of 455 kHz, and during the sweep time it covers a bandwidth of 30 kHz. A TTL dual VCO chip (SN74LS124N) is used for this purpose as shown in Figure 16. Using an external component, either a capacitor or a crystal, and

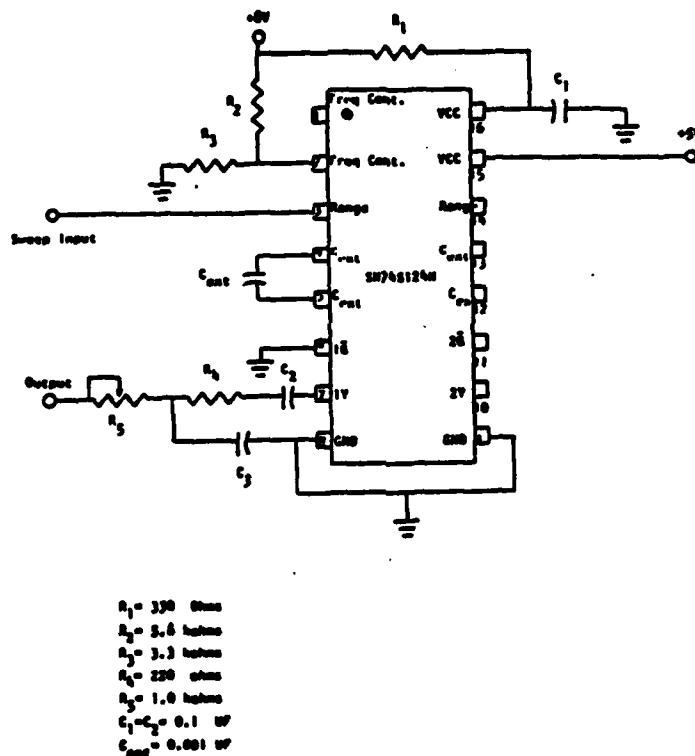


FIGURE 16: The Voltage-Controlled Oscillator Circuit

two voltage-sensitive inputs, the proper VCO can be designed. One of these voltage-sensitive inputs is for the frequency control and the other one for

the frequency range [18]. Several graphs are provided in the data book for proper design. The voltage at pin 2 determines which graph to use and the sweep voltage at pin 3 determines the variation in frequency of the oscillator. An external capacitor connected between pin 4 and pin 5 sets the center frequency of the oscillator. This device can be operated with a single 5 V supply. However, a set of supply voltages and ground pins (16, 15, 9 and 8) is provided for the oscillator and associated frequency-control circuits so an effective isolation can be accomplished in the system. The value of the external capacitance is obtained from:

$$f_0 = 5 \times 10^{-4} / C_{\text{ext}}$$

$$f_0 = 455 + 15 = 470 \text{ kHz}$$

Hence,

$$C_{\text{ext}} = .001 \text{ UF}$$

The output at pin 7 is lowpass filtered so that the high-frequency spikes at the transition time on the square wave (output) are suppressed. The 1 K ohm trim pot ( $R_5$ ) enables us to adjust the magnitude of the VCO output which is applied to the balanced modulator (mixer).

To produce the 455 kHz signal, the sweep voltage is 2.73 V and it linearly changes to the value of 2.28 V which is needed to produce the 485 kHz signal. The output of the VCO is set to 150 mV<sub>p</sub> which then is applied to the mixer. Note that the specifications and the graphs given for SN745124N in the data book [18] are not consistent with the experimental results. Hence, some experiments were needed to achieve the proper results.

### 3.5 Sweep Generator

As explained in Section 3.2, sweep rates of 15 and 30 seconds were chosen. Hence, a linear ramp must be generated to control the VCO and the widband amplifier gain. The scheme most often used to generate a linear ramp is to pump constant current into a capacitor using a transistor. This transistor is switched off and on by a pulse generator whose width is equal to the sweep rate (i.e., 15 and 30 seconds).

The ramp generator used here (Figure 17a) is designed with the same principle in mind, except an RC network with very long time constant is used instead of a constant current generator. The capacitor would eventually charge to 15 volts, but (due to the long time constant) by the time the 15th or 30th second is reached, the capacitor has only charged up to approximately 2 V. RC networks charge up exponentially and the early portions of the exponential are quite linear. This is how the linear ramp is generated for this spectrum analyzer. The transistor shown in Figure 17a is merely used as a switch, and the 470 UF capacitor is charged via 180 K ohm resistor for the 15 seconds

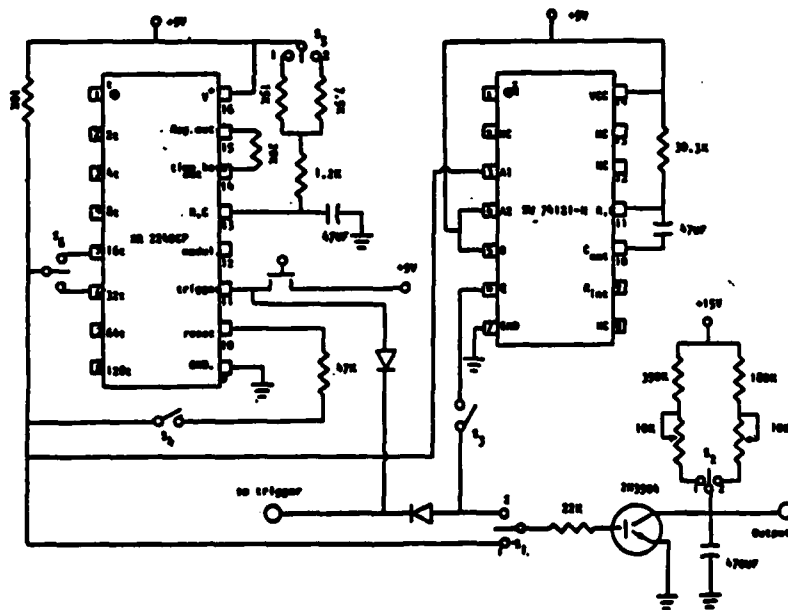


FIGURE 17a: The Sweep Generator Circuit

sweep and via a 390 K ohm resistor for the 30 second sweep. When the transistor is off this capacitor charges up and discharges very rapidly through the emitter when the transistor switches to the on state. Time constants are set so that the ramp reaches 1.78 V.

To turn the transistor off and on, a timer chip (XR2240CP) is used. This chip is a programmable complex pulse pattern generator. The width of the pulses is dictated by two parameters. The first parameter depends on the RC combination connected to pin 13 as shown in Figure 17a. Pins 1 through 8 are binary counter outputs which can be shorted together to a common pull-up resistor. The second parameter depends on the combination of these pins to be connected together as the output. The combined outputs will be low as long as any one of them is low. For example, if pins 1, 5 and 6 are connected together, the "low state" time will be  $(1 + 16 + 32)RC$ . The output is high until a 5 V pulse is applied to the trigger pin (pin 11). The output stays low until the time for which the chip is programmed. The output waveform will be monostable if pin 10 (reset) is not connected to the output bus, otherwise it will be astable. The astable mode is used to create continuous sweep.

To produce a continuous sweep, a SW74121-N one-shot trigger is used. For a pulse train applied to the input, the output stays low until the high-to-low transition occurs. Then the output goes high for a time duration set by an RC combination at pins 10, 11 and 14. For our need, RC is set so that a pulse train with 16 seconds period applied at the input causes the output to stay low for 15 seconds and high for 1 second to allow time for transients to die out and distinguish between the sweeps. Hence, the output of the transistor in this mode will be zero V for 1 second, followed by a 15 second sweep.

When an x-y recorder or a digital system is used to record the output of the spectrum analyzer, some type of marker is needed to distinguish the start

of a sweep. Also, for the continuous-sweep mode, markers between sweeps are needed to denote starts and ends of the individual sweeps. The trigger pulse at pin 11 of the timer and the 1-second high state pulse at the output of the one-shot trigger are connected to the post amplifier, and as these pulses occur they show up at the output of the spectrum analyzer to indicate the start and the end of the sweeps.

The pulse trains for 15-second single and continuous sweeps are shown in Figures 17b-d. For 30-second sweeps all the pulse widths are doubled. The single and continuous sweeps are set as follows:



FIGURE 17b: Output of the Timer for Single Sweep

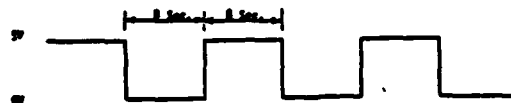


FIGURE 17c: Output of the Timer for Continuous Sweep



FIGURE 17d: Output of the One Shot (74121) for Continuous Sweep

15 sec sweep  $S_2$  at 2,  $S_6$  at 2

30 sec sweep  $S_2$  at 1,  $S_6$  at 1

One switch is used for setting these modes. Another switch sets for single or continuous sweeps.

Single sweep:  $S_4$  closed,  $S_1$  at 1,  $S_3$  at 1,  $S_3$  open

Continuous sweep:  $S_1$  and 2,  $S_5$  at 2,  $S_3$  closed

The output of the ramp generator (collector of the transistor) for a 15 second single sweep was recorded on an x-y recorder and is shown in Figure 17e. This shows that the ramp is quite linear.

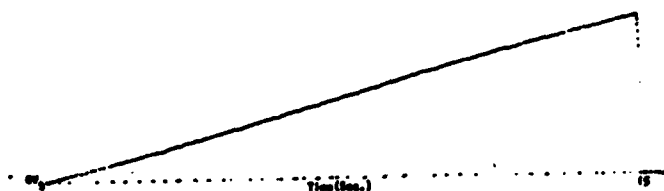
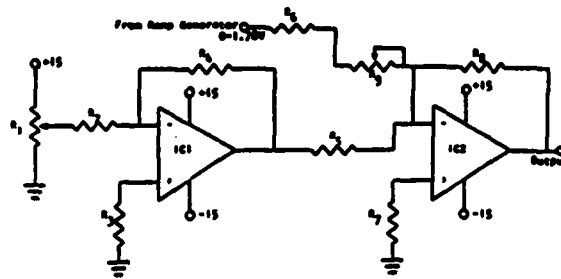


FIGURE 17e: The Ramp Generator Output

### 3.6 VCO Input Voltage Network

As was explained in Section 3.3, the proper linear changing of frequencies by the VCO requires a linear ramp which starts at 3.73 V and decreases to 2.28 V on pin 3 of the VCO. The sweep generator produces a ramp which starts at zero V and increases to 1.78 V. Hence a network was needed which takes 0 - 1.78 V as the input and produces 2.73 - 2.28 V as the output. Figure 18 shows such a network. The 10 K trim pot ( $R_1$ ) sets the output voltage when  $V_s = 0$  and the 20 K trim pot ( $R_0$ ) sets the output voltage at the end of the sweep. By adjusting these trim pots the desired 2.73 - 2.28 V range is produced.



$R_1=10$  Kohms  
 $R_2=0.2$  Kohms  
 $R_3=R_4=R_5=0.7$  Kohms  
 $R_6=12$  Kohms  
 $R_7=0.7$  Kohms  
 $R_8=15$  Kohms  
 $R_9=00$  Kohms  
 $IC1=IC2=1/2MC1496$

FIGURE 18: The Sweep Network for VCO

### 3.7 The Mixer

Balanced modulators are designed for use where the output voltage is a product of an input voltage (signal) and a switching function (carrier). The MC1496 is such an IC which also provides great carrier suppression, amplitude modulation and FM detection. This chip has excellent carrier suppression of -65 dB at 500 kHz; it also has adjustable gain. Carrier suppression is defined as the ratio of each sideband output to carrier output for the carrier and signal voltage levels used. Carrier suppression is very dependent on carrier input level. A low value of the carrier does not fully switch the upper switching devices inside the chip, which results in lower signal gain and therefore lower carrier suppression. A high carrier level results in unnecessary carrier feedthrough, which also reduces the suppression. Carrier feedthrough is independent of signal level, hence carrier suppression can be maximized by operating with large signal levels. However, a linear operation must be maintained in the signal-input transistor pair or harmonics of the modulating signal will be generated and appear in the device output as

spurious sidebands of the suppressed carrier [19]. Cookbook designs for AM modulators are available as test circuits [19]. The output signal is taken from pins 6 and 9 for either balanced or single-ended mixing. The circuit of the mixer is shown in Figure 19. Figure 20 shows the rated output gain vs frequency for the MC1496. Detailed considerations are given in the Motorola Linear Handbook [19].

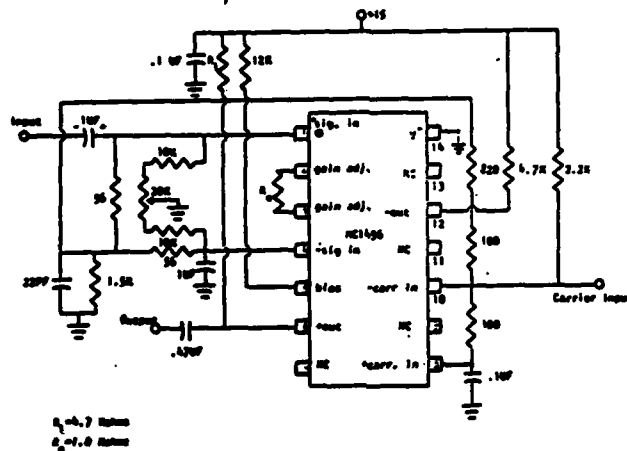


FIGURE 19: The Mixer Circuit

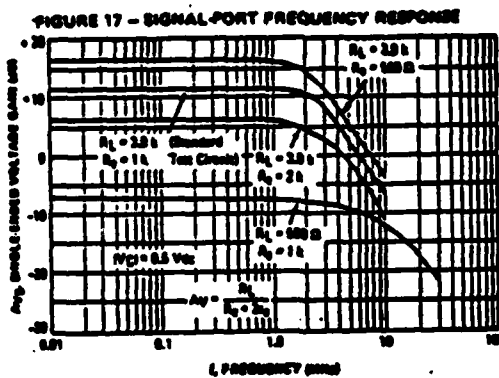
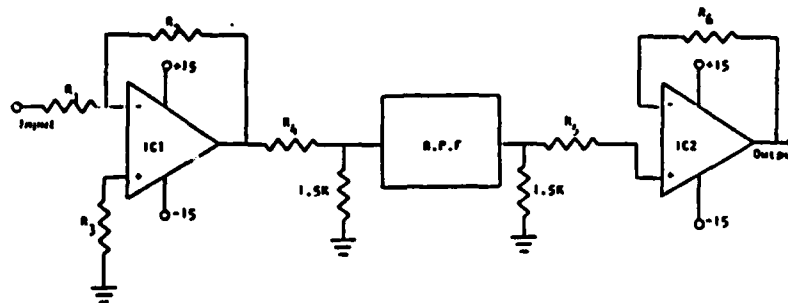


FIGURE 20: Gain Characteristics of the Mixer (MC1496)

### 3.8 The Amplifier and the First Filter

At the mixer output the signal has been amplified twice: in the pre-amplifier with 20 dB gain and in the mixer with about 12 dB gain. The modulated signal from the output of the mixer is further amplified by 23.5 dB in an inverting amplifier (IC1 of Figure 21). The signal is then passed through a 3 kHz-wide BPF centered at 455 kHz. This cleans up the signal



$R_1=10$  Kohms  
 $R_2=150$  Kohms  
 $R_3=10$  Kohms  
 $R_4=1.0$  Kohms  
 $R_5=12$  Kohms  
 $R_6=72$  Kohms  
IC1=LF357  
IC2=5534  
B.P.F. 455KHz @30Hz BW

**FIGURE 21: The Amplifier, Filter and Buffer**

somewhat before it is applied to the resolution filter, as shown by testing. This filter introduces a loss of about 5 dB. It also requires input and output impedance matching. These matches are provided by the two 1.5 K ohms resistors connected to its input and output. At this point the signal is to be applied to the swept-gain stage. To avoid any loading problems between the filter and the swept gain stage a simple voltage follower (buffer) (IC2 of Figure 21) was placed between these two stages.

### 3.9 The Swept-Gain Stage

A probing radar encounters strong echoes from the surface of the ground or ice, and antenna reflections and other internal system reflections associated with the radar are also strong. These reflections occur at the lower end of the returned frequency spectrum due to their relatively short ranges. These echoes are not of interest in probing systems; it is desirable to suppress them. One way to accomplish this task is by using an amplifier with adjustable gain capability. By this method the low-frequency signals are amplified less than those at higher frequencies.

An MC1590 IC is a wideband amplifier with automatic gain control capability. Two parameters set the gain reduction: the value of the AGC resistor connected to pin 2, and the voltage level applied to this resistor [19]. Figure 22a shows the gain reduction vs AGC voltage achieved for two different AGC resistors. The gain reduction variation is more linear for larger AGC

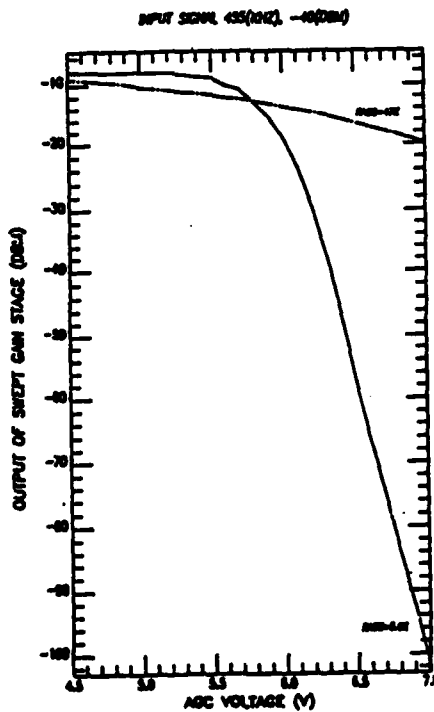


FIGURE 22a: Wide Band Amp. Response

resistances as shown in Figure 22a. Therefore, as the sweep is going by, the proper values of the voltage can be applied to the AGC input which results in the automatic gain reduction for different returned frequencies. Figure 22b shows the complete circuit for this wideband amplifier.

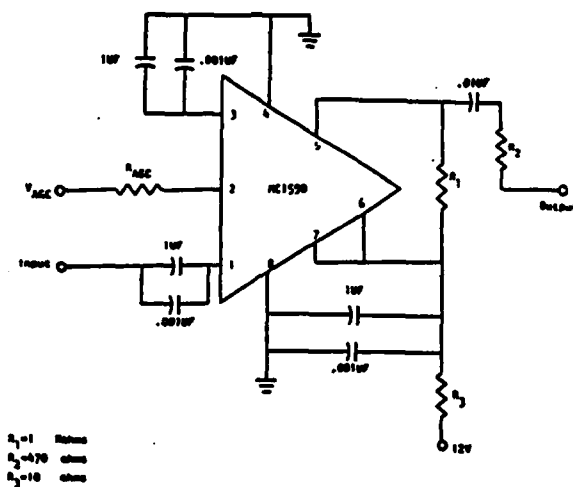
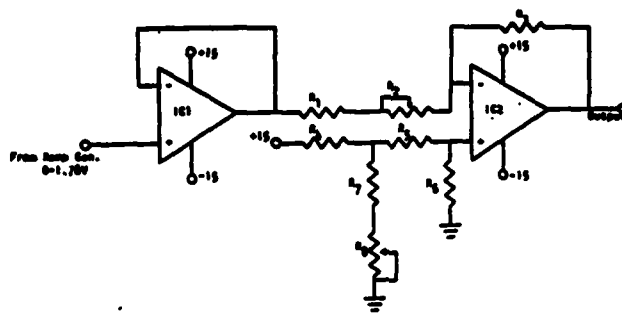


FIGURE 22b: The Wideband Amplifier (Swept Gain Stage)

### 3.10 The AGC Signal Network

Assume that it is required to suppress the returned signal spectrum from dc to 10 kHz and have a constant gain value from 10 kHz to 30 kHz. Figure 22a shows that the above requirement is met if the AGC voltage is set at 6 volts at the start of the sweep and linearly descends to 4.5 V at the end of the ramp. To produce the proper linear AGC voltage ramp, the same idea as in Section 3.5 is employed. Although the network used for this purpose is a little different from the one in 3.5, their functions are identical. This network is shown in Figure 23. The first op-amp (IC1) acts as a buffer with the ramp generator output which linearly changes from 0 to 1.78 V as its input. The



$R_1=5.6$  Kohms  
 $R_2=50$  Kohms  
 $R_3=2.2$  Kohms  
 $R_4=5.6$  Kohms  
 $R_5=12$  Kohms  
 $R_6=100$  Kohms  
 $R_7=2.2$  Kohms  
 $R_8=50$  Kohms  
 IC1=IC2=1/2MC1498

FIGURE 23: The Sweep Network for AGC

second op-amp takes this 0 - 1.78 V ramp as its input and produces the proper voltages at its output. The trim pot ( $R_8$ ) at the non-inverting input sets the output voltage when the input is zero V. The other trim pot ( $R_2$ ) sets the output voltage when the input voltage has reached 1.78 V. Since the input signal changes linearly, the output signal does the same.

### 3.11 The Resolution Filter

At this point in the system the signal from the IF port of the radar has been amplified, shifted to a frequency near 455 kHz, and amplified again with a controlled gain variation. The output of the swept-gain stage is now ready to go through the resolution filter shown in Figure 24. This is a crystal-tuned 200 Hz-bandwidth filter centered at 455 kHz. The tuneable filter explained in Section 2.1 is the combination of VCO, mixer and filter. The filter introduces a loss of about 3 dB, and both input and output ports should be matched by 600 ohm impedances. To avoid any loading problems between the swept-gain stage and the filter and aid in impedance matching of the input

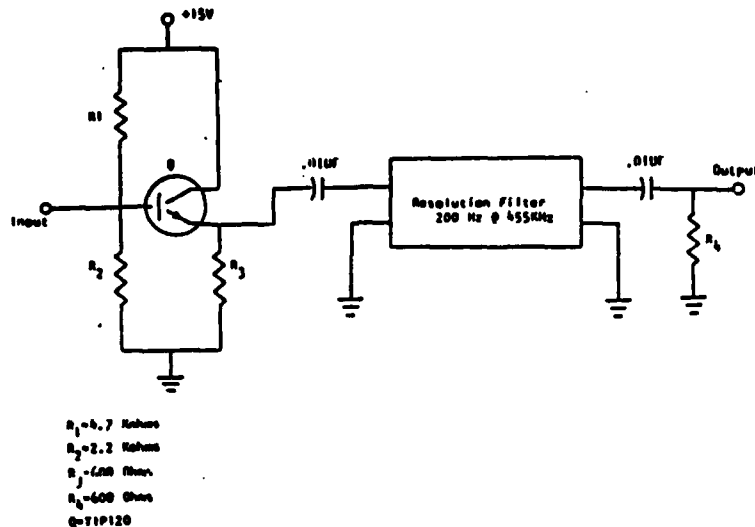
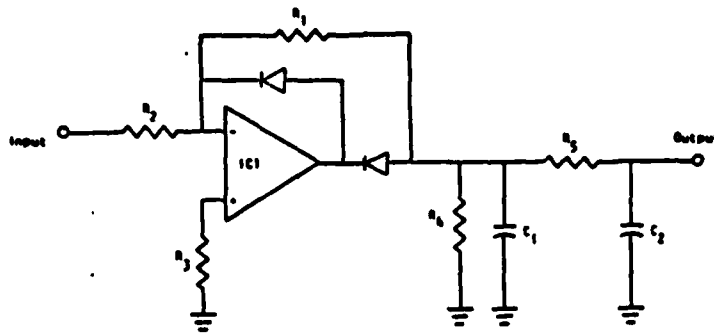


FIGURE 24: The Circuit of the Resolution Filter

port, a buffer (0) is used which has an output impedance of 600 ohms. The output port is matched by connecting a 600 ohm resistor ( $R_4$ ) between the output and ground. The exact specifications of this filter (frequency response, loss, etc.) are not available. The 3 dB loss figure was once measured with an HP spectrum analyzer in the laboratory. Due to the narrow passband of this filter, it is very difficult to obtain a frequency response graph by applying discrete signals to the input and measuring the output. The said HP analyzer was not available at the time of writing to produce an x-y recording of the filter frequency response.

### 3.12 The Detector

The circuit diagram of the detector is shown in Figure 25. The op-amp network is a unity gain of half-wave rectifier. A signal at 455 kHz was applied to the input of the rectifier and the output was monitored. The input level was attenuated to a level for which no output was observed. This minimum level of the input signal to the detector was measured at -38 dBm.



$R_1 = 10 \text{ K ohms}$   
 $R_2 = 10 \text{ K ohms}$   
 $R_3 = 0.7 \text{ K ohms}$   
 $R_4 = 10 \text{ K ohms}$   
 $R_5 = 100 \text{ K ohms}$   
 $IC1 = LF357$   
 $C_1 = 220 \text{ PF}$   
 $C_2 = .122 \text{ PF}$

FIGURE 25: The Detector Circuit

The values of  $R_4$  and  $C_1$  were chosen so that  $R_4 C_1 \ll 1/\omega_m$  and  $R_4 C_1 \ll 1/\omega_c$  where  $\omega_m$  and  $\omega_c$  are the maximum modulation and carrier frequencies in rad/sec.

$$\omega_c = 2\pi(455) \text{ K rad/sec}$$

$$\omega_m = 2\pi(30) \text{ K rad/sec}$$

Hence,

$$.35 \text{ } \mu\text{sec} \ll R_4 C_1 \ll 5.3 \text{ } \mu\text{sec}$$

Let  $R_4 C_1 = 2.5 \text{ } \mu\text{sec}$  and let  $R_4 = 10 \text{ K ohms}$ ; hence

$$C_1 = 250 \text{ pF.}$$

Choose  $C_1 = 220 \text{ pF.}$  Hence,

$$R_4 C_1 = 2.2 \text{ } \mu\text{sec.}$$

A small amount of carrier-frequency ripple is present on the detected waveform. This ripple can be eliminated by using a lowpass filter. The combination of  $R_5$  and  $C_2$  is this lowpass filter. Let's choose 10 Hz as the cutoff frequency;  $f_0 = 10 \text{ Hz.}$

$$f_0 = 1/2\pi R_f C_2,$$

choose  $R_f = 100 \text{ K ohms}$

Then

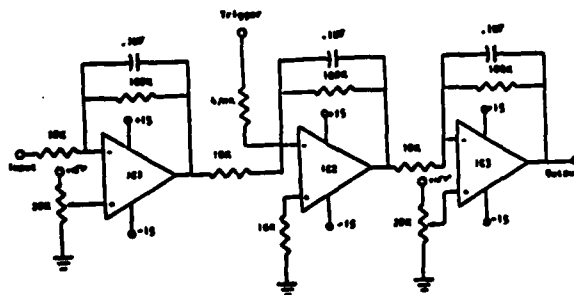
$$C_2 = .159 \mu\text{F},$$

choose  $C_2 = .122 \mu\text{F}$

which is the parallel combination of  $.1 \mu\text{F}$  and  $220 \text{ PF}$ . So, the actual cutoff is at  $f_0 = 13 \text{ Hz}$ .

### 3.13 The Post Amplifier

The post amplifier required a gain of 100; it amplifies the dc detector output. Figure 26 shows the circuit diagram for this amplifier. The first stage (IC1) amplifies the signal by a factor of 10. This amplified signal is further amplified by a factor of 10 at the second stage (IC2). In this stage the trigger signal (markers) is amplified by a factor of .21 and is added to the signal from the first stage. The last stage is a unity-gain amplifier; its output is the final output of the spectrum analyzer. The trim pots at the first and last stage are used to null out any dc offset introduced by the detector or the op-amps. The  $.1 \mu\text{F}$  capacitors connected across each feedback resistor serve to further lowpass filter the signal from the detector or any coupled signal from other components.



62-102-102-000000

FIGURE 26: The Post Amplifier

## 4.0 RESULTS

Once the spectrum analyzer had been built, several tests were done to check its performance. A dynamic range test was run to establish the lowest and highest detectable signal levels. In addition, several simple probing experiments were performed and the results compared against those obtained using an HP3585A spectrum analyzer.

### 4.1 Dynamic Range Test

As discussed in Section 3.2, we would like to be able to detect signal levels from -100 dBm to -10 dBm in probing experiments. In order to measure the lowest detectable signal level, the following was done:

- (1) A step attenuator was connected between the input port of the spectrum analyzer and a sine-wave generator.
- (2) A 25 kHz at -60 dBm signal was applied to the spectrum analyzer and the attenuation factor was set at zero.
- (3) The output of the spectrum analyzer was monitored on an oscilloscope.
- (4) The attenuation factor was increased each time the output was seen on the scope as the deflection of the beam.
- (5) More and more attenuation factor was added until no deflection was seen on the scope.
- (6) At an input level of -98 dBm a deflection of about 7 mV was seen on the scope.

Therefore, -98 dBm is the lowest detectable signal level. The highest detectable signal level depends on the saturation level of the total amplifiers and the linear operation region of the components. The maximum input level to the mixer should not exceed 5.0 V (rms), hence the input level to the spectrum

analyzer should not exceed 0.5 V (rms). One might set the highest detectable signal level at .3 V or 0.0 dBm in order to guarantee detection.

#### 4.2 Frequency Calibration

In order to calibrate for the location of a signal on the frequency axis, a -50 dBm tone at different frequencies was applied to the input of the spectrum analyzer. The result of this test is illustrated in Figure 27. It is clearly shown that the lower frequency signals are attenuated and from about 11 kHz to 32 kHz the magnitude of the signals is equal. This is due to the swept gain stage which was discussed in Section 3.9.

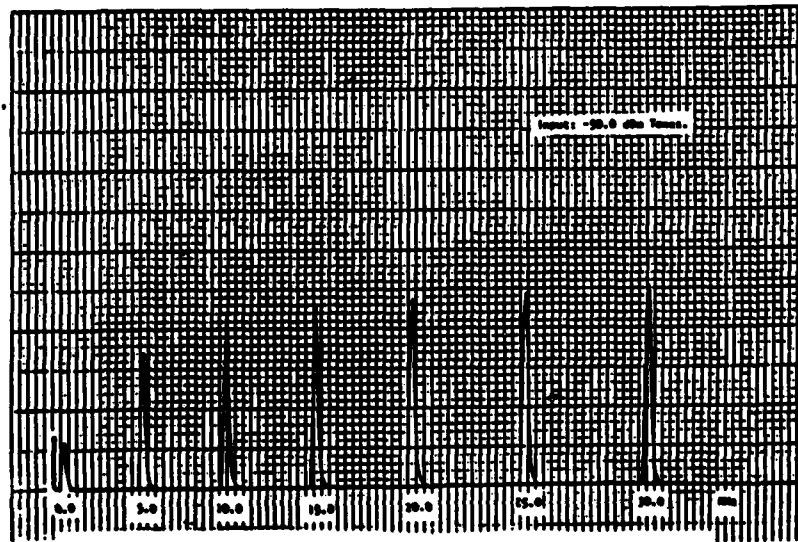


**FIGURE 27: Spectrum Analyzer Response**

The response of the VCO is not exactly linear. As seen in Figure 27, the spacing between 0 and 5 kHz is smaller than 25-30 kHz. Hence, there is a need for some calibration scheme in order to know the exact location of a signal.

From this figure we can see that the spacing between 0 and 32 kHz is 80 small divisions. The location of each tone versus the number of the small division on which it falls is known. This information is plotted in Figure 28 as the actual data. A power curve fit ( $y = ax^b$ ) is used to fit this data into a curve. The result is that  $a = 1.7627$ ,  $b = 1.0836$ , and the coefficient of determination is .9999 which indicates how well the curve fits the data. This equation is also plotted in Figure 28.

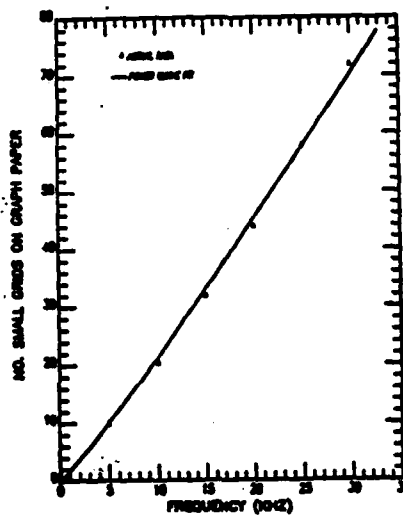


FIGURE 28: Frequency Calibration Curve

To see how this curve can be used to determine the frequency of a signal, all the operator has to do is use a piece of 7 x 10 inch graph paper. The settings on the x-y recorder will be up to him. Then two numbers should be counted from the x-y plot: first, the number of small grids for a complete sweep; second, the number of the grid corresponding to the desired signal. Then use the relation:

$$\frac{(\# \text{ of the grid for the signal}) \times 80}{\# \text{ of the grids for a total sweep}}$$

Whatever this number comes out to be, locate it on the vertical axis of Figure 28, then use the curve to find the corresponding frequency value from the horizontal axis.

To check the accuracy of this scheme, a delay line return (using the sled-scat system) with the FM rate of 225 Hz was plotted using an HP3585A spectrum analyzer with a resolution bandwidth of 300 Hz. The same signal was plotted with the designed spectrum analyzer with a resolution bandwidth of 200 Hz. Using the frequency calibration scheme, the frequency of the delay line return was calculated to be 19.35 kHz compared to 19.56 kHz measured on the HP3585A spectrum analyzer. In later experiments this difference is related to the range discrepancy. Figures 29a and b show these two recorded delay line signals.

#### 4.3 Probing Experiments and Results

This spectrum analyzer is built for probing experiments. Thus, to check its performance some probing results are needed. At the time of these experiments, our low frequency probing radar had not been put together yet, therefore the sled-scat radar system was used. Operating at X-band with about

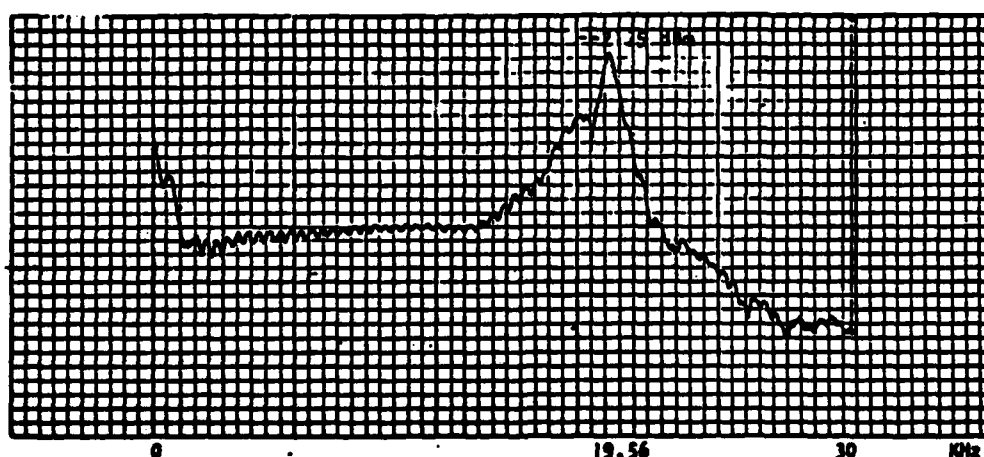


FIGURE 29a: Delay Line Return (by the HP3585A Spectrum Analyzer)  
Res. BW - 300 Hz,  $f_m = 225$  Hz

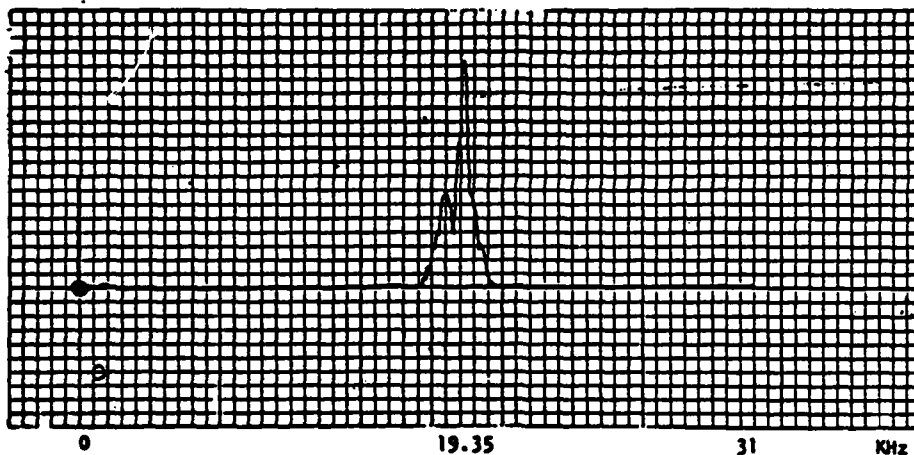


FIGURE 29b: Delay Line Return (by the Spectrum Analyzer)  
Res. BW = 200 Hz,  $f_m = 224$  Hz

15 dBm transmitting power, this is not a suitable probing system, but in order to accommodate these probing experiments, the following setup was arranged. With  $0^\circ$  incidence angle and antenna height of 4.3 m (distance between the dish and the ground), the ground reflection was recorded by the two spectrum analyzers. Figures 30a and b illustrate the results produced by these two spectrum analyzers. The difference between the measured and calculated

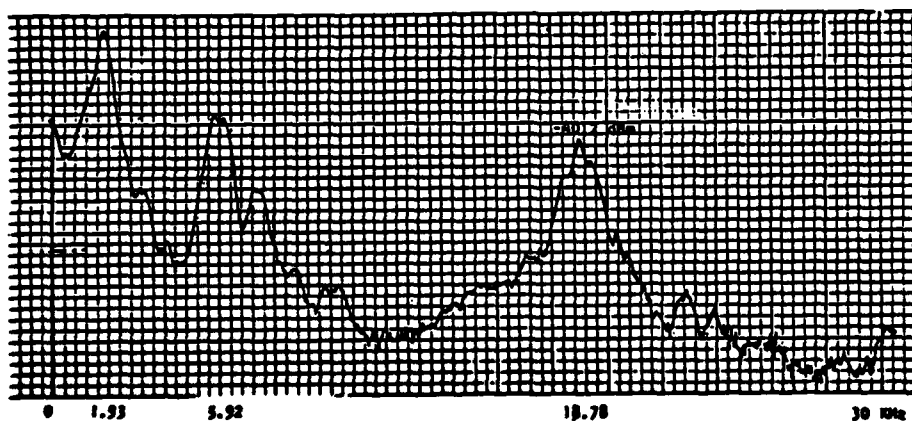
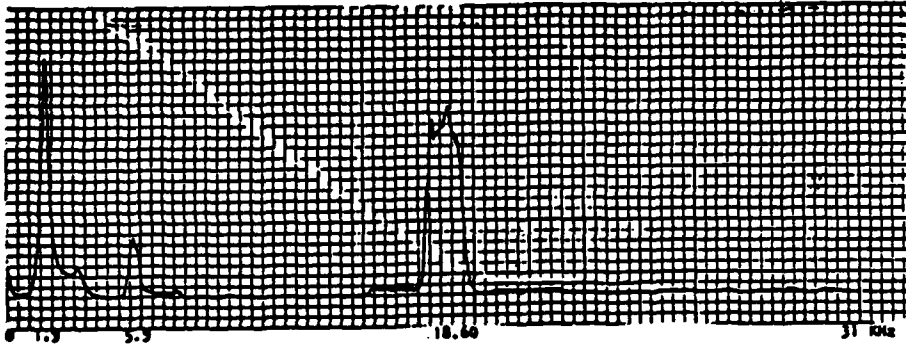


FIGURE 30a: Ground Return (by the HP3585A Spectrum Analyzer)



**FIGURE 30b: Ground Return (by the Spectrum Analyzer)**

frequencies is 180 Hz. However, the frequency discrepancy for the system and the antenna reflections are only 30 Hz and 20 Hz, respectively (FM rate was set at 111 Hz).

A plastic bucket 82.5 cm tall was placed, upside down, on the ground under the antenna. The reflections from the plastic surface and the ground were recorded by the two spectrum analyzers (see Figures 31a and b). From Figure 31b the height of the bucket can be determined using the frequency difference between the two signal returns. The height is calculated to be 94.6 cm. Compared to the actual height of 82.5 cm, this is a difference of 8.1 cm.

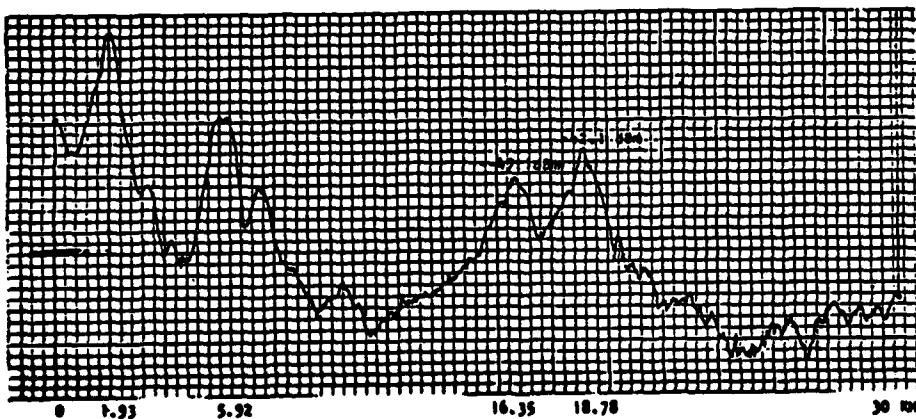


**FIGURE 31a: Bottom of the Bucket and the Ground Returns (by the HP3585A Spectrum Analyzer)**

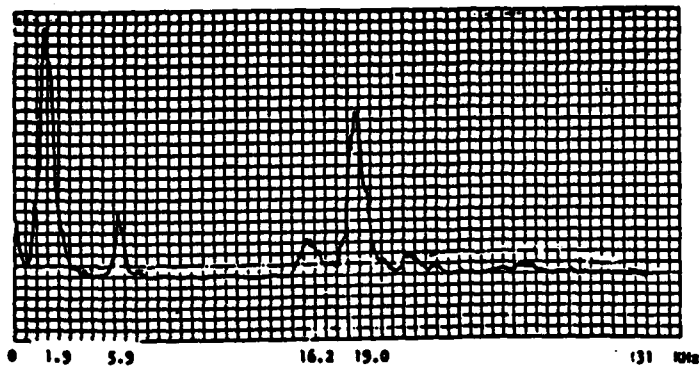


**FIGURE 31b: Bottom of the Bucket and the Ground Returns  
(by the Spectrum Analyzer)**

For the next experiment, the plastic surface of the bucket was covered by putting 3.5-inch-thick concrete blocks on it. The results of this experiment were plotted by both of the spectrum analyzers and are shown in Figures 32a and b. The ground reflection is smaller than the concrete surface reflection because the signal from the ground attenuates through the concrete twice and the concrete had been sitting outside, so it was not very dry. This increases its dielectric constant which is about 8 when dry.

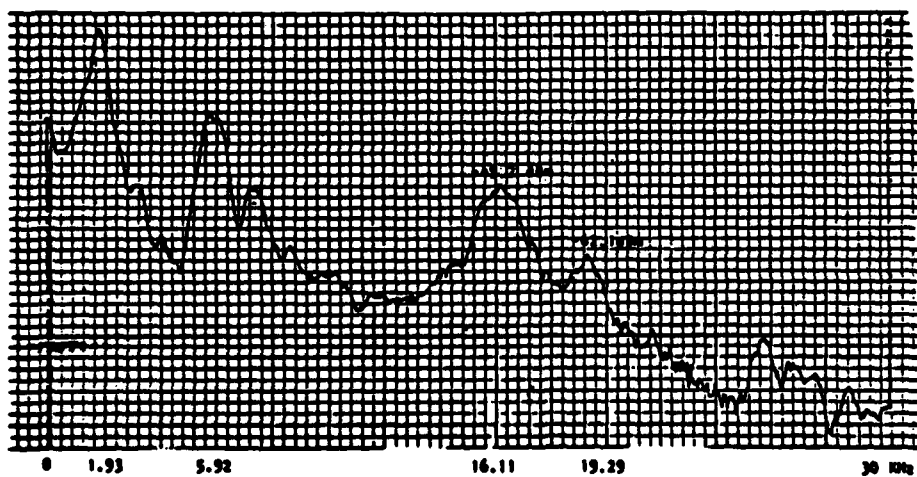


**FIGURE 32a: Concrete and Metal Returns (by the HP3585A Spectrum Analyzer)**

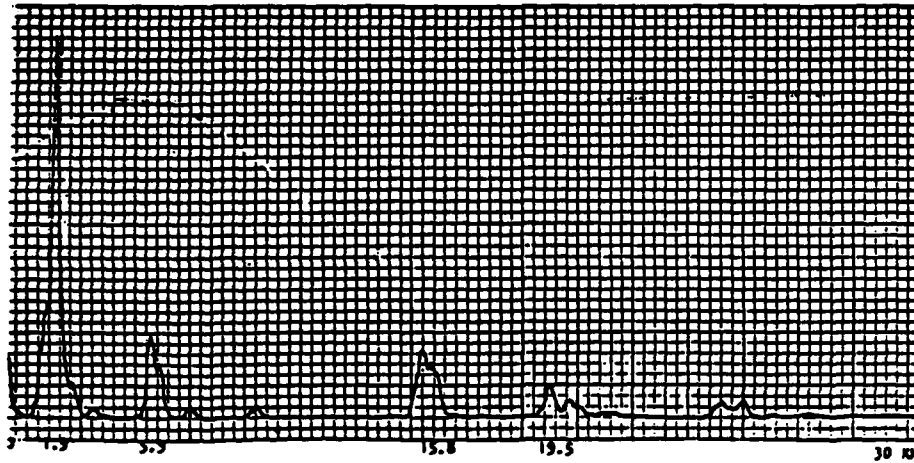


**FIGURE 32b: Concrete and Ground Returns (by the Spectrum Analyzer)**

Next, a flat metal plate (aluminum) was laid on the ground. The metal plate reflection now replaced the ground reflection. This plate reflection is higher than the ground reflection due to the higher reflectivity of the metal plate. Figures 33a and b illustrate these results. The experiment setup with the bucket only is shown in Figure 34, and with bucket and concrete in Figure 35.

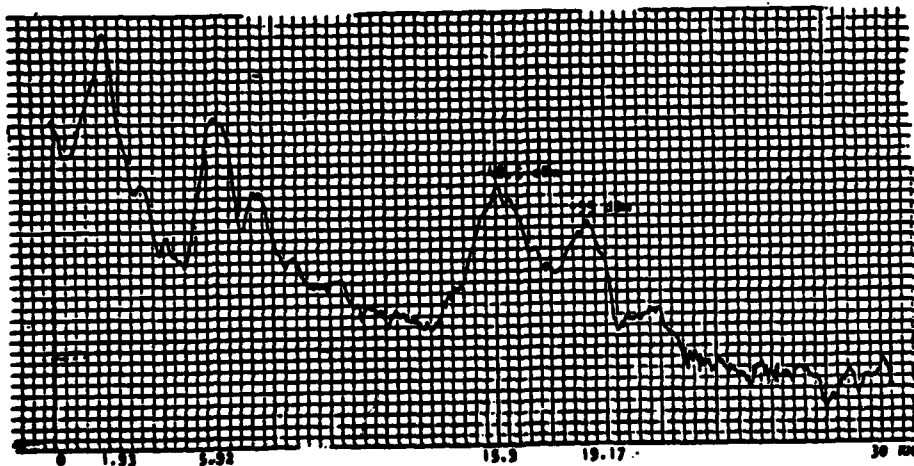


**FIGURE 33a: Concrete and Metal Plate Returns (by the HP3585A Spectrum Analyzer)**

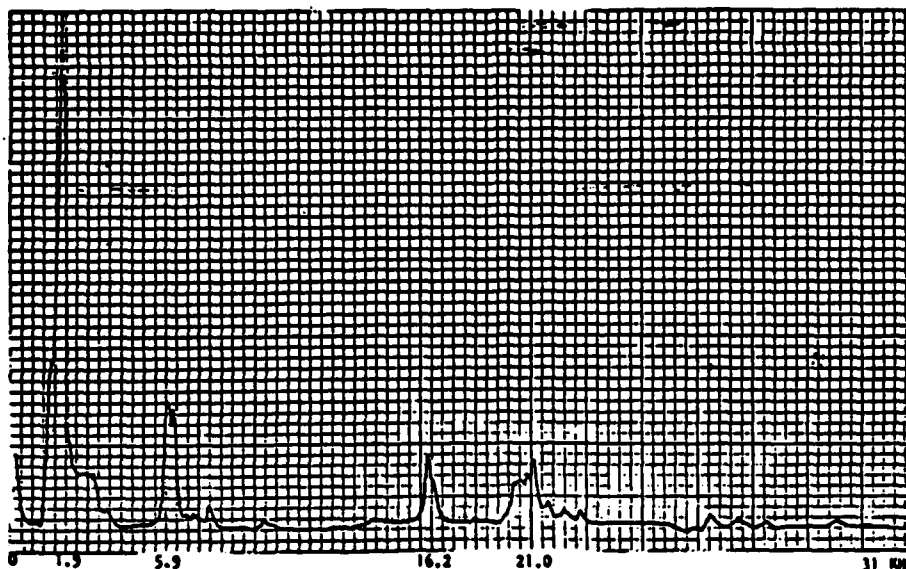


FIGURE 33b: Concrete and Metal Plate Returns (by the Spectrum Analyzer)



FIGURE 34: The Experiment Set-Up Showing the Bucket and Antenna

## 5.0 CONCLUSION AND RECOMMENDATIONS

A spectrum analyzer used in probing experiments was specified. The theoretical concepts of an FM-CW radar system commonly used in probing experiments were discussed to enhance understanding the function of this spectrum analyzer as the device to interpret the output signal of the radar.



**FIGURE 35: The Experiment Set-Up Showing the Bucket and the Concrete and the Antenna**

An overall block diagram design was put together and each of these blocks was later designed in detail and built. Necessary modifications to these designs were made throughout the course of building the spectrum analyzer. In order to verify that the specifications were met, several tests were made. The instrument performed satisfactorily both in the test for dynamic range and in the simple probing tests when compared with an HP3585A spectrum analyzer. A scheme was devised to calibrate the frequency of any signal. This scheme proved to be very accurate for calibrating lower frequency portions of the sweep and at higher portions it was accurate within about  $\pm 250$  Hz of the actual value. Overall this design seems to be operating well within its specified values.

For future modifications to this design, a more stable and linear VCO is recommended. Also, for more accurate frequency calibration, a pulse train which produces spectral lines (spikes) at every 2 kHz and with a null greater than 30 kHz could be superimposed on the x-y plot of all produced spectra. A logarithmic amplifier could also be added to the design in order to provide both linear and logarithmic scale measurements of the produced spectra.

## REFERENCES

- [1] Finkelshetin, M., "Radar Remote Sensing of Sea Ice Thickness," Intercosmos Council, Academy of Science, Moscow, USSR, no date given.
- [2] Burrell, G.A. and L. Peters, Jr., "Pulse Propagation in Lossy Media Using the Low-Frequency Window for Video Pulse Radar Application," Proc. IEEE, vol. 67, no. 7, July 1979, pp. 981-990.
- [3] Elbert, A.C. and J.D. Young, "The Development and Field Testing of a New Locator for Buried Plastic and Metal Utility Lines," Rec. Transport. Res. Bd. 56th Annual Meeting, Washington, D.C., January 1977.
- [4] Young, J.D. and R. Caldecott, "Underground Pipe Detector," U.S. Patents 4,967,282 and 4,062,010, March 7, 1977.
- [5] Young, J.D. and R. Caldecott, "A Portable Detector for Plastic Pipe and Other Underground Objects," Electroscience Lab Report 404X.1, Ohio State Univ., Columbus, Ohio, September 1973.
- [6] Lundien, J.R., "Determining Presence, Thickness and Electrical Properties of Stratified Media Using Swept Frequency Radar," U.S. Army Engineer Topographic Lab Technical Report M-72-4, Vicksburg, Mississippi, November 1972.
- [7] Moore, R.K., C. Nasser and R.G. Onstott, "Probing of Concrete for Void Detection Using an L-band FM Radar," RSL TR 3488-0038-2, U. of Ks. CRINC, Lawrence, Kansas, November 1981.
- [8] Barakat, N., et al., "Electromagnetic Sounder Experiments at the Pyramids of Giza," Joint Ainsams University, Cairo, ARE and Stanford (California) Res. Inst., National Science Foundation Report, May 1975.
- [9] Chan, L.C., D.L. Moffatt and L. Peters, Jr., "A Characterization of Sub-surface Radar Targets," Proc. IEEE, vol. 67, July 1979, pp. 991-1000.
- [10] Fowler, J.C., "Subsurface Reflection Profiling Using Ground-Probing Radar," SME Reprint 79-341, October 1979.
- [11] Annan, A.D. and J.L. Davis, "Impulse Radar Sounding in Permafrost," Radio Science, Vol. 11, no. 4, April 1976, pp. 383-394.
- [12] Skolnik, M.I., Introduction to Radar Systems, N.Y.: McGraw-Hill, 1980.
- [13] Moore, R.K., Chapter 9, Manual of Remote Sensing, Falls Church, VA: American Society of Photogrammetry, 1975.
- [14] Moore, R.K., S. Gogineni and Y.H. Lin, "Preliminary Feasibility Study of a Broadband FM Radar for Ground Probing," RSL TR 361-1, U. of Ks. CRINC, Lawrence, Kansas, February 1980.
- [15] Moore, R.K., C. Nasser and R.G. Onstott, "Use of Broadband FM Radar in Ground Probing," RSL TR 3488-0038-1, U. of Ks. CRINC, Lawrence, Kansas, October 1981.
- [16] Shanmugan, K.S., Digital and Analog Communication Systems, New York: John Wiley and Sons, 1979.
- [17] Moore, R.K., "Sweeping Rates for Spectrum Analyzer," RSL TR 331-6, U. of Ks. CRINC, Lawrence, Kansas, May 1980.
- [18] TTL Data Book for Engineers, 2nd edition, Texas Instruments, Inc., 1976.
- [19] Motorola Linear Data Book, Phoenix, Ariz.: Motorola, Inc., 1979.

END

FILMED

12-84

DTIC